STUDYING TURBULENCE USING DOPPLER-BROADENED LINES: VELOCITY COORDINATE SPECTRUM

A. Lazarian

Department of Astronomy, University of Wisconsin, Madison, US

D. Pogosyan

Physics Department, University of Alberta, Edmonton, Canada
ApJ, accepted 26 July 2006

ABSTRACT

We discuss a new technique for studying astrophysical turbulence that utilizes the statistics of Doppler-broadened spectral lines. The technique relates the power Velocity Coordinate Spectrum (VCS), i.e. the spectrum of fluctuations measured along the velocity axis in Position-Position-Velocity (PPV) data cubes available from observations, to the underlying power spectra of the velocity/density fluctuations. Unlike the standard spatial spectra, that are function of angular wavenumber, the VCS is a function of the velocity wave number $k_v \sim 1/v$. We show that absorption affects the VCS to a higher degree for small k_v and obtain the criteria for disregarding the absorption effects for turbulence studies at large k_v. We consider the retrieval of turbulence spectra from observations for high and low spatial resolution observations and find that the VCS allows one to study turbulence even when the emitting turbulent volume is not spatially resolved. This opens interesting prospects for using the technique for extragalactic research. We show that, while thermal broadening interferes with the turbulence studies using the VCS, it is possible to separate thermal and non-thermal contributions. This allows a new way of determining the temperature of the interstellar gas using emission and absorption spectral lines.

Subject headings: turbulence – ISM: general, structure – MHD – radio lines: ISM.

1. INTRODUCTION

Astrophysical fluids are usually turbulent and the turbulence is magnetized. This ubiquitous turbulence determines the transport of heat and cosmic rays in the interstellar medium (see Elmegreen & Falgarone 1996, Stutzki 2001, Narayan & Medvedev 2001, Schlickeiser 2002, Cho et al. 2003, Lazarian 2006a) the intra-cluster medium (Inogamov & Sunyaev 2003, Sunyaev, Norman & Bryan 2003), processes of star formation (see McKee & Tan 2002, Elmegreen 2002, Larson 2003, Ballesteros-Paredes et al. 2006), and interstellar chemistry (see Falgarone 1999, Falgarone et al. 2006). An extended list of interstellar processes governed by turbulence is given in Elmegreen & Scalo (2004).

Using a statistical description is a nearly indispensable strategy when dealing with turbulence. The big advantage of statistical techniques is that they extract underlying regularities of the flow and reject incidental details. Kolmogorov description of unmagnetized incompressible turbulence is a statistical one. For instance, it predicts that the difference in velocities at different points in a turbulent fluid increases on average with the separation between points as a cube root of the separation, i.e. $|\delta v| \sim l^{1/3}$. In terms of the direction-averaged energy spectrum this gives the famous Kolmogorov scaling $E(k) \sim 4\pi k^2 P(k) \sim k^{5/3}$, where $P(k)$ is a *3D* energy spectrum defined as the Fourier transform of the correlation function of velocity fluctuations $\langle \delta v(\mathbf{x}) \delta v(\mathbf{x} + \mathbf{r}) \rangle$. In this paper we use $\langle ... \rangle$ to denote the ensemble averaging procedure[1].

The velocity energy spectrum $E(k)dk$ characterizes how much energy resides in the interval of scales $k, k + dk$. At large scales l which correspond to small wave-numbers k (i.e. $l \sim 1/k$) one expects to observe features reflecting energy injection. At small scales one should see the scales corresponding to sinks of energy. In general, the shape of the spectrum is determined by a complex process of non-linear energy transfer and dissipation. For Kolmogorov turbulence the spectrum over the inertial range, i.e. the range where neither energy injection nor energy dissipation are important, is characterized by a single power law and is, therefore, self-similar. Other types of turbulence, i.e. the turbulence of non-linear waves or the turbulence of shocks, are characterized by different power laws and therefore can be distinguished from the Kolmogorov turbulence of incompressible eddies. Substantial advances in our understanding of the scaling of compressible MHD turbulence (see reviews by Cho & Lazarian (2005), and references therein) allows us to provide a direct comparison of theoretical expectations with observations.

Recovering the velocity spectra from observations is a challenging problem that has been studied for more than half a century. Indeed, the first measurements were obtained with the velocity in the 50s (see von Hoerner 1951, Munch 1958). While the centroids were widely used to study turbulence in molecular clouds (see Kleiner & Dickman 1985, Dickman & Kleiner 1985, Miesch & Scalo 1995, 1999) the recent theoretical work and numerical testing (Lazarian & Esquivel 2003, Esquivel & Lazarian 2005, Ossenkopf et al. 2006) show that velocity centroids can reliably recover

---

[1] The relation between the ensemble averaging and more common spatial averaging is discussed in Monin & Yaglom (1975). We address the related issues throughout the paper when we discuss the practical implementations of our statistical technique.

velocity spectra only for subsonic or mildly supersonic turbulence.

If turbulence is supersonic, the recovering of its velocity spectrum is possible with the Velocity Channel Analysis (VCA), introduced in LP00. This technique has already been successfully used to study turbulence (see Stanimirovic & Lazarian 2001). However, the VCA is just one way to use the general description of fluctuations in the Position-Position Velocity space (henceforth PPV), presented in LP00. One can also study fluctuations along the *velocity coordinate.* The appropriate formulas that relate the spectra along the velocity axis in the PPV volume to the underlying velocity spectrum were derived in the Appendix of LP00. However, the utility and big advantages of such a study have been realized only recently. The corresponding technique was termed the Velocity Coordinate Spectrum (henceforth VCS) in Lazarian (2004) and the first examples of the practical application of VCS are presented in Lazarian (2005, 2006).

We feel that the importance of this new technique calls for a more rigorous analytical study. Therefore one of the goals of the present paper is to provide more solid mathematical foundations for the VCS technique. Even more important is to find out to what extent the absorption affects the VCS. As the absorption takes place in real space, we derive our formulas in real space while the study in LP00 was done in the Fourier space.

The structure of our paper is as follows. In §2 we introduce the central object of our study, namely, the 1D correlation function of PPV intensities in the presence of absorption. We consider both high resolution (pencil beam) and finite resolution. In §3 we relate the correlations of velocity and density in real space and the correlations in PPV space. We revisit Lazarian & Pogosyan (2004, henceforth LP04) and provide an improved discussion of the dominance of velocity and density correlations to PPV correlations. In addition, we define transformations that reveal hidden symmetries in the PPV space and extend the asymptotics of PPV correlations that we obtained in our earlier studies. In §4 we consider the case of an optically thin medium and obtain the expressions for the VCS for both narrow and wide beams. We discuss the transition from one regime to another as we probe different spatial scales of turbulence. In §5 we derive the criteria for the VCS to be applicable to the observational data with self-absorption. A comparison of the VCS with other techniques of turbulence studies, a brief discussion of the simplifications of the model, as well as an outline of the prospects of the technique are given in §6. The summary is provided in §7. Appendixes are important parts of our paper. The list of our notations is given in Appendix A. We discuss the practical averaging of spectral line data in Appendix B. The fundamentals of the PPV statistics, i.e. PPV correlation functions and spectra, are derived in Appendix C. A discussion of PPV power spectra and the transformation that reveals the symmetries between the spatial and velocity coordinates is provided in Appendix D.

2. CORRELATIONS ALONG VELOCITY COORDINATE IN PPV

2.1. *The Problem: Simplified Approach*

The main object of our present study is a volume of turbulent gas or plasma (a "cloud"). Turbulent motions of the gas, and its inhomogeneous distribution lead to fluctuations of intensity in the observed Doppler shifted emission or absorption lines. Our goal is to relate the statistical measures that can be obtained through spectral line observations to the underlying properties of the turbulent cascade. In what follows, we concentrate on the case of the emission study, while keeping in mind that the general formalism presented in this paper can be easily extended to absorption studies.

We assume that the cloud extent along the line of sight S is much smaller than the distance from the volume to the observer. This allows us to use the geometry of parallel lines of sight. Each line of sight can then be labeled by a two-dimensional position vector $\mathbf{X}$ on the cloud image, which together with z coordinate along the line of sight specifies the three-dimensional position vector $\mathbf{x} = (\mathbf{X}, z)$. Henceforth, following the convention adopted in LP00 and LP04 we denote by the capital bold letters the two dimensional position-position vectors reserving small bold letters for vectors of three dimensional spatial position. Replacing z coordinate by the observationally available z-component of gas velocity gives us a vector $(\mathbf{X}, v)$ in PPV cube. (Where the convergence of lines of sight is essential, cf. Chepurnov & Lazarian, 2006, v should be treated as the radial coordinate.)

In this paper we study the fluctuations in PPV space in the velocity coordinate along the fixed line of sight, taking into account the effects of self absorption of gas and the finite angular resolution of the telescope. Let us first introduce the problem in a simplified form, disregarding the effects of telescope resolution (cf. §2.2, §6.2.2). A possible statistical measure of the fluctuations of emission intensity $I_{\mathbf{X}}(v)$ is the structure function

$$\mathcal{D}(\mathbf{X}, v_1, v_2) \equiv \left\langle [I_{\mathbf{X}}(v_1) - I_{\mathbf{X}}(v_2)]^2 \right\rangle \quad , \tag{1}$$

which is the variance of the difference between intensities at two velocities v_1, v_2 along the same line of sight $\mathbf{X}$. We stress that the measure (1) is available for the *infinite* spatial resolution of an instrument, while for the finite resolution an averaging over the neighboring lines of sight with the instrumental beam should be performed (see §2.2).

The intensities $I_{\mathbf{X}}(v)$ are affected by both the turbulence and the absorption. As in LP04, to quantify these effects consider the standard equation of radiative transfer (Spitzer 1978)

$$dI_\nu = -g_\nu I_\nu ds + j_\nu ds \ , \quad ds = -dz \quad , \tag{2}$$

with the absorption coefficient $g_\nu = \alpha(\mathbf{x})\rho(\mathbf{x})\phi_v(\mathbf{x})$ and the emissivity $j_\nu = \epsilon\rho(\mathbf{x})\phi_v(\mathbf{x})$ are taken proportional to the density of atoms with velocity v that corresponds to the frequency ν. This density is given by $\rho(\mathbf{x})\phi_v(\mathbf{x})$, where $\rho(\mathbf{x})$ is the spatial density of atoms and $\phi_v(\mathbf{x})$ is the fraction of atoms that have velocity v. The turbulent motions affect the velocity distribution. Indeed, the line-of-sight velocity v of the atom at the position $\mathbf{x}$ is a sum of z-components

of the regular gas flow (e.g., due to galactic rotation) $v_{gal}(\mathbf{x})$, the turbulent velocity $u(\mathbf{x})$ and the residual component due to thermal motions. This residual thermal velocity $v - v_{gal}(\mathbf{x}) - u(\mathbf{x})$ has a Maxwellian distribution, so

$$\phi_v(\mathbf{x})\mathrm{d}v = \frac{1}{(2\pi\beta)^{1/2}} \exp\left[-\frac{(v - v_{gal}(\mathbf{x}) - u(\mathbf{x}))^2}{2\beta}\right]\mathrm{d}v \quad, \tag{3}$$

where $\beta = \kappa_B T/m_a$, m_a being the mass of atoms. If the temperature tends to zero, the function becomes a δ-function, that prescribes the velocity distribution that is determined by non-thermal velocities.

As shown in LP04 the solution of Eq. (2) is

$$I_{\mathbf{X}}(v) = \epsilon \int_0^{\rho_s} dY_v \mathrm{e}^{-\alpha Y_v} = \frac{\epsilon}{\alpha}\left[1 - \mathrm{e}^{-\alpha\rho_s(\mathbf{X},v)}\right] \quad, \tag{4}$$

where

$$\rho_s(\mathbf{X}, v) \equiv \int_0^S \rho(z')\phi_v(z')dz' \quad. \tag{5}$$

is the density of *images* of the emitting atoms in PPV space, which henceforth we shall refer to as the PPV density. Again, following the convention in LP00 and LP04, we use the subscript s to distinguish the quantities in $(\mathbf{X}, v)$ coordinates from those in $(\mathbf{X}, z)$ coordinates. As the result, Eq. (1) can be written as

$$\mathcal{D}(v_1, v_2) = \frac{\epsilon^2}{\alpha^2}\left\langle\left[e^{-\alpha\rho_s(\mathbf{X},v_1)} - e^{-\alpha\rho_s(\mathbf{X},v_2)}\right]^2\right\rangle \quad, \tag{6}$$

where, for the sake of simplicity, we omitted the label $\mathbf{X}$. This is what we shall do for the rest of the paper, wherever this does not cause a confusion.

The effects of turbulence are imprinted on $\mathcal{D}(v_1, v_2)$ through $\rho_s(\mathbf{X}, v)$. The PPV density $\rho_s(\mathbf{X}, v)$ depends on the real density of gas $\rho(\mathbf{X}, z)$ and on velocity of gas particle $v(\mathbf{X}, z)$.

2.2. Effects of Finite Angular Resolution

Realistic observations have a finite angular resolution. The emission intensity measured by a telescope is $\int d\mathbf{X_1} B(\mathbf{X_1})I_{\mathbf{X_1}}(v_1)$, where $B(\mathbf{X_1})$ is the beam of the instrument, assumed to be centered on the line of sight at $\mathbf{X_1} = 0$. The explicit introduction of the beam was avoided in LP00 and LP04 as those papers dealt with slices of data for which spatial resolution was essential. For the case of studies of fluctuations along the velocity coordinate, meaningful results may be obtained for spatially unresolved eddies as well.

Since integration commutes with taking ensemble average, the structure function of the beam-smeared signal is given by

$$\mathcal{D}(v_1, v_2) \equiv \int d\mathbf{X_1} B(\mathbf{X_1})\int d\mathbf{X_2} B(\mathbf{X_2})\left\langle[I_{\mathbf{X_1}}(v_1) - I_{\mathbf{X_1}}(v_2)][I_{\mathbf{X_2}}(v_1) - I_{\mathbf{X_2}}(v_2)]\right\rangle \quad, \tag{7}$$

that is a generalization of Eq. (1).

Using Eq. (4) and a short hand notation $\rho_{ij} = \rho_s(\mathbf{X}_i, v_j)$, we can express $\mathcal{D}(v_1, v_2)$ via PPV density in the following form

$$\mathcal{D}(v_1, v_2) = \frac{\epsilon^2}{\alpha^2}\int d\mathbf{X_1} B(\mathbf{X_1})\int d\mathbf{X_2} B(\mathbf{X_2}) \times$$
$$\left\langle e^{-\alpha(\rho_{11}+\rho_{21})}\left[1 - e^{-\alpha(\rho_{12}-\rho_{11})} - e^{-\alpha(\rho_{22}-\rho_{21})} + e^{-\alpha(\rho_{12}-\rho_{11}+\rho_{22}-\rho_{21})}\right]\right\rangle \quad. \tag{8}$$

The idea behind writing the structure function in this form is to notice that the term in square brackets depends on the difference between PPV densities at different velocities, but along the same line of sight, $\rho_{21} - \rho_{22}$ and $\rho_{11} - \rho_{12}$, while the prefactor, $\rho_{11} + \rho_{21}$, is evaluated at the same velocity, although between different lines of sight. This makes Eq. (8), still fully general, particularly convenient for studying scaling behavior at small velocity separations.

To proceed further we need to consider some limiting cases and approximations. At sufficiently small $v = v_1 - v_2$, one can expand the terms in the brackets into the power series

$$\mathcal{D}(v) \sim \epsilon^2 \int d\mathbf{X_1} B(\mathbf{X_1})\int d\mathbf{X_2} B(\mathbf{X_2}) \times$$
$$\left\langle e^{-\alpha(\rho_{11}+\rho_{21})}\left[(\rho_{12} - \rho_{11})(\rho_{22} - \rho_{21}) + O\left(\alpha\Delta\rho^3\right) + O\left(\alpha^2\Delta\rho^4\right)\right]\right\rangle \quad, \tag{9}$$

where we assumed homogeneity of correlation functions in the velocity direction. As we discuss in Appendix B this is not a necessary condition for the theory formulation, but we use it to simplify both our discussion and notations.

In LP04 [2] we argued, that factoring out the averaging over the "absorption window" $e^{-\alpha(\rho_{11}+\rho_{12})}$

$$\mathcal{D}(v) \sim \epsilon^2 \int d\mathbf{X_1} B(\mathbf{X_1})\int d\mathbf{X_2} B(\mathbf{X_2}) \times$$
$$\left\langle e^{-\alpha(\rho_{11}+\rho_{21})}\right\rangle\left[\left\langle(\rho_{12} - \rho_{11})(\rho_{22} - \rho_{21})\right\rangle + \left\langle O\left(\alpha\Delta\rho^3\right)\right\rangle + \left\langle O\left(\alpha^2\Delta\rho^4\right)\right\rangle\right] \quad. \tag{10}$$

---

[2] Our consideration is similar to the one we advanced in LP04 for the two dimensional structure function of intensity. There, however, the role of velocity v and angular R directions were reversed.

provides a good approximation for studying the onset of the absorption effects.

In the case of an isotropic beam and homogeneous statistics the last expression becomes

$$\mathcal{D}(v) \sim \epsilon^2 \int RdR\, B^2(R)\, W_{abs}(R) \left[d_s(R, v) - d_s(R, 0) + \langle O\left(\alpha \Delta \rho^3\right)\rangle + \langle O\left(\alpha^2 \Delta \rho^4\right)\rangle \right] \quad, \tag{11}$$

where $R = |\mathbf{X_1} - \mathbf{X_2}|$, the PPV structure function is

$$d_s(R, v) = \langle [\rho_s(\mathbf{X_2}, v_2) - \rho_s(\mathbf{X_1}, v_1)]^2 \rangle \quad, \tag{12}$$

the absorption window W_{abs} is

$$W_{abs}(R) = \langle e^{-\alpha[\rho_s(\mathbf{X_1}, v_1) + \rho_s(\mathbf{X_2}, v_1)]} \rangle \quad, \tag{13}$$

and

$$B^2(R) = 2\pi \int d\mathbf{X_+} B(\mathbf{X_+} + \mathbf{R}/2) B(\mathbf{X_+} - \mathbf{R}/2), \quad \mathbf{X_+} = (\mathbf{X_1} + \mathbf{X_2})/2 \quad. \tag{14}$$

Eq. (11) provides the foundations of the formalism for finite resolution studies.

2.3. *High Resolution Limit*

The formalism is significantly simplified in the limit of infinitely high angular resolution, $B(\mathbf{X}) = \delta(\mathbf{X})$. The criterion for neglecting the beam spread depends on the properties of the turbulence.

For infinitely high (henceforth, *high*) resolution Eq. (8) becomes

$$\mathcal{D}(v) = \frac{\epsilon^2}{\alpha^2} \langle e^{-2\alpha\rho_1} \left[1 - e^{-\alpha(\rho_2 - \rho_1)} \right]^2 \rangle$$
$$\approx \frac{\epsilon^2}{\alpha^2} \langle e^{-2\alpha\rho_1} \rangle \langle \left[1 - e^{-\alpha(\rho_2 - \rho_1)} \right]^2 \rangle \quad. \tag{15}$$

where we have omitted a now irrelevant first spatial index in ρ, $\rho_i \equiv \rho(0, v_i)$. At the velocity scales both large enough for the beam width to be neglected (which allows to set R to zero), and small enough for the series expansion to be accurate

$$\mathcal{D}(v) \sim \epsilon^2 W_{abs}(0) \left[d_s(0, v) + \alpha \langle (\rho_1 - \rho_2)^3 \rangle + \frac{\alpha^2}{12} \langle (\rho_1 - \rho_2)^4 \rangle + O(\alpha^4) \right] \quad. \tag{16}$$

The Eqs (11), (16) provide the basis for the subsequent discussion of the short scale limit of statistical descriptors and the conditions under which the absorption start to play a role. They establish the link between observable fluctuations of intensity along the line of the velocity coordinate, which are characterized here by $\mathcal{D}(v)$, and statistical descriptors of PPV density ρ_s, namely, $d_s(R, v)$ (see Eq. (12)).

3. FLUCTUATIONS IN REAL SPACE AND PPV SPACE

This section presents the ground work in relating the correlation and structure functions in the PPV space and the relevant statistical descriptors of the velocity and density in the emitting turbulent volume.

3.1. *Statistical measures of velocity, density and PPV density*

3.1.1. *Correlations and spectra in real space*

It is well known that in the presence of magnetic field turbulence becomes axisymmetric in the reference frame related to the *local* direction of magnetic field (see discussion in Cho, Lazarian & Vishniac 2002 and references therein). However, as we have discussed earlier (see LP00, LP04), to a large extent it is possible to use isotropic statistics of density and velocity when dealing with observations. Briefly, this is related to the fact that the observations are performed in the *global* system of reference related to the mean magnetic field. In this system of reference the anisotropy is rather mild and spectra in directions parallel and perpendicular to the magnetic field have the same scaling. These considerations were successfully tested using synthetic observations with the data cubes obtained through direct 3D MHD simulations (Esquivel et al. 2003).

The fact above permits us to use the standard isotropic statistical measures like structure function, correlation function and spectra (see Monin & Yaglom 1976) to describe both the velocity and density correlations in the turbulent cloud under study. In what follows, we use the statistically isotropic (see Lazarian 1995 for a more general case) correlation function of the xyz-space density field $\rho(\mathbf{x})$

$$\xi(r) = \xi(\mathbf{r}) = \langle \rho(\mathbf{x})\rho(\mathbf{x} + \mathbf{r}) \rangle \quad, \tag{17}$$

as well as the correlation function of the density fluctuations $\delta\rho = \rho - \langle \rho \rangle$

$$\tilde{\xi}(r) = \langle \delta\rho(\mathbf{x})\delta\rho(\mathbf{x} + \mathbf{r}) \rangle = \xi(r) - \langle \rho \rangle^2 \quad. \tag{18}$$

At zero lag, $\xi(0) = \langle \rho^2 \rangle$ is the second moment of the field. At large separations the correlation function provides the square of the mean value, $\xi(\infty) \to \bar{\rho}^2$, while $\tilde{\xi}(\infty) \to 0$.

In addition, we use the density structure function

$$d(r) = \langle (\rho(\mathbf{x} + \mathbf{r}) - \rho(\mathbf{x}))^2 \rangle \quad , \tag{19}$$

and the density power spectrum

$$P(\mathbf{k}) = \int d\mathbf{r} e^{i\mathbf{k}\mathbf{r}} \xi(\mathbf{r}) \quad or \quad P(\mathbf{k}) = -\tfrac{1}{2} \int d\mathbf{r} e^{i\mathbf{k}\mathbf{r}} d(\mathbf{r}) \quad . \tag{20}$$

The utility of using both structure and correlation functions can be illustrated with density fluctuations. An essential difference between the two is that, while the value of the structure function at some scale r, $d(r)$, is determined by the integrated power of fluctuations over smaller scales $r' \leq r$, the value of the correlation function $\xi(r)$ reflects the integral of the power over scales $r' \geq r$. Therefore, the correlation functions are more appropriate to use for spectra where most power is at increasingly small scales (Monin & Yaglom 1975), in particular for power-law spectra $P(k) \sim k^n$, for $n > -3$. Following LP00 and LP04, we call such spectra "shallow". In contrast, the "steep" power spectra, for which $n < -3$ and most of the power is on the large scales, are more robustly described by the structure function.

For exact power law spectra with steep index, the correlation function is not formally well defined due to divergent contribution from large scales [3], while for shallow index the structure function diverges due to small scale power. However, as we discussed in LP04, if the appropriate cut-offs at small and/or large scales are introduced, both descriptors can be used simultaneously and relate simply to each other

$$d(r) = 2\left[\xi(0) - \xi(r)\right] \quad , \quad \tilde{\xi}(r) = \tfrac{1}{2}\left[d(\infty) - d(r)\right] \quad . \tag{21}$$

In this case $d(\infty) = 2\left(\xi(0) - \bar{\rho}^2\right) = 2\tilde{\xi}(0)$.

For a shallow power law spectrum the correlation function is a decaying power law $\tilde{\xi}(r) \propto r^{-\gamma}$ with $\gamma > 0$, while for a steep power-law spectrum the structure function $d(r) \propto r^{-\gamma}$, is a rising power-law with $\gamma < 0$ (see Monin & Yaglom 1975, and numerical examples in Esquivel & Lazarian 2005). The relation between the spectral index n of $P(k)$ and the index γ of structure (for a steep spectrum) or correlation (for a shallow spectrum) functions is straightforward:

$$\text{spectral index} = \gamma - \text{dimensionality of space} . \tag{22}$$

In this notation Kolmogorov turbulence in 3D has $\gamma = -2/3$ and the spectral index of $P(k)$, $n = -11/3$. The usually quoted Kolmogorov $-5/3$ index corresponds to the direction averaged spectrum, namely to $4\pi k^2 P(k)$.

We also use a structure function to characterize the turbulent velocity. Since only the z-component of the velocity field is available, we just need

$$D_z(\mathbf{r}) = \langle (u_z(\mathbf{x} + \mathbf{r}) - u_z(\mathbf{x}))^2 \rangle \quad . \tag{23}$$

Unlike the density for which both shallow and steep cases can be realized depending on the ratio of fluid viscosity and resistivity (see Lazarian, Vishniac & Cho 2004), and Mach number (see Beresnyak, Lazarian & Cho 2005), the velocity field scaling is always steep (see Cho, Lazarian & Vishniac 2003). The latter we write as $D_z(r) \propto r^m$, $m > 0$. [4]

3.1.2. Correlations in PPV

In what follows we assume 2D statistical homogeneity and isotropy of $\rho_s(\mathbf{X}, v)$ in the $\mathbf{X}$-direction over the image of a cloud. Homogeneity and isotropy in $\mathbf{X}$ causes the mean density to depend only on velocity, while the correlation functions depend only on the magnitude of separation between two sky directions $R = |\mathbf{R}| = |\mathbf{X_1} - \mathbf{X_2}|$. Then, in PPV space the mean density is

$$\bar{\rho}_s(v_1) = \langle \rho_s(\mathbf{X}_1, v_1) \rangle \quad , \tag{24}$$

and the correlation functions of the density and, closely related, density fluctuations $\delta\rho_s(\mathbf{X}_1, v_1) = \rho_s(\mathbf{X}_1, v_1) - \bar{\rho}_s(v_1)$ are

$$\xi_s(R, v_1, v_2) \equiv \langle \rho_s(\mathbf{X}_1, v_1) \rho_s(\mathbf{X}_2, v_2) \rangle \quad , \tag{25}$$

$$\tilde{\xi}_s(R, v_1, v_2) \equiv \langle \delta\rho_s(\mathbf{X}_1, v_1) \delta\rho_s(\mathbf{X}_2, v_2) \rangle = \xi(R, v_1, v_2) - \bar{\rho}_s(v_1)\bar{\rho}_s(v_2) \quad . \tag{26}$$

For PPV statistics the structure functions are

$$d_s(R, v_1, v_2) = \langle [\rho_s(\mathbf{X}_1, v_1) - \rho_s(\mathbf{X}_2, v_2)]^2 \rangle \quad , \tag{27}$$

$$\tilde{d}_s(R, v_1, v_2) = \langle [\delta\rho_s(\mathbf{X}_1, v_1) - \delta\rho_s(\mathbf{X}_2, v_2)]^2 \rangle = d_s(R, v_1, v_2) - [\bar{\rho}_s(v_1) - \bar{\rho}_s(v_2)]^2 \quad . \tag{28}$$

Here we have maintained the notation which highlights the symmetries of the correlation and structure functions. The conditions under which the homogeneity along a velocity direction is fulfilled are formulated in Appendix B. For the rest of the paper we assume that they are satisfied and we assume that the PPV correlation and structure functions depend only on the velocity difference v. In Section 3.5 we discuss some asymptotic symmetries between $\mathbf{X}$ and v directions.

[3] For very steep spectra, i.e. for $n < -5$, even structure functions fail to keep in check the contribution from large scale gradients and to properly reflect the turbulence statistics (Monin & Yaglom, see also examples in Cho & Lazarian 2004, 2005). We obtain such steep power spectra for fluctuations of intensity along the velocity coordinate and the problems that this entails are addressed below.

[4] Note the difference in the signs of γ that we use for density with steep spectra and m used for velocity structure functions. This difference is somewhat unfortunate, but in case of density where both steep and shallow spectra are possible, it allows us to write $\sim r^{-\gamma}$ scaling universally for both the correlation and structure functions.

3.1.3. *Relation between PPV and real space correlations*

The PPV correlations can be expressed via real space velocity and density correlations using the set of assumptions that was employed in LP00 and LP04 (see also Appendix C). If the gas is confined in an isolated cloud of size S and the galactic shear over this scale is neglected, the zero-temperature correlation function is (see Appendix C)

$$\xi_s(R,v) \propto \int_{-S}^{S} dz \left(1 - \frac{|z|}{S}\right) \frac{\xi(r)}{D_z^{1/2}(\mathbf{r})} \exp\left[-\frac{v^2}{2D_z(\mathbf{r})}\right], \tag{29}$$

where, assuming for the sake of simplicity that the velocity field is solenoidal, the structure function of the z-components of velocity is (see LP04)

$$D_z(\mathbf{r}) = Cr^m \left[1 + \frac{m}{2}\left(1 - z^2/r^2\right)\right] \quad, \tag{30}$$

where C is a normalization constant. We keep the vector notation, as, unlike the correlation function of the scalar density field, the structure function of even isotropic vector field depends not just on r, but also on the angle with the z-axis (via z/r) (see Monin & Yaglom 1975). In terms of R and z, a useful explicit expression is

$$D_z(\mathbf{r}) = C \left(R^2 + z^2\right)^{m/2-1} \left([1 + m/2]R^2 + z^2\right) \quad. \tag{31}$$

If the turbulent energy cascades from a scale larger or equal to the cloud size S, $D_z(\mathbf{r})$ is growing up to the scale of the cloud S at which the velocity structure function saturates at the value $D_z(S) = CS^m$. Note, that a somewhat complicated prefactor entering Eq. (C6) is omitted in Eq. (29), which is justified as we are interested in the functional dependence of ξ_s rather than its amplitude. This expression is obtained by substituting ρ_s given by Eq. (5) into the definition of the correlation function (25) and performing averaging over the Gaussian distribution of the turbulent velocity field $u(\mathbf{x})$, contained in $\phi_v(\mathbf{x})$ (see Appendix C).

For the studies of turbulence in the presence of a regular flow, e.g. the galactic shear velocity v_{gal}, one should replace v in the exponent in Eq. (29) by $v - v_{gal}$ (see LP00 and LP04). We found that neglecting the regular flow provides an adequate approximation for studies in a wide range of circumstances. Besides isolated clouds, this includes observations in directions of high galactic latitude, but also the case of HI in the Galactic plane, if we focus on small scale phenomena. Indeed, the velocity gradient arising from the Galactic rotation is ~ 0.7 km/s/50pc and decreases linearly to shorter scales. At the same time turbulent relative motions of HI are expected to be 20 km/s at $50pc$ and scale as $r^{1/3}$. Thus, even if turbulent scaling saturates at $S \sim 50pc$, for considering linear scales $r < S$, or, correspondingly, in velocity direction $v < D_z^{1/2}(S) \sim 20$ km/s, it is justifiable to neglect coherent shearing motions arising from galactic rotation. If turbulence is extended to ever larger scales the region of validity of the approximation extends until turbulent velocities equate with the shearing motion. This scale, denoted λ in LP00, is equivalent to the "cloud" size[5] S.

The effect of thermal motions is described by the convolution of correlation functions evaluated at a vanishing temperature with a thermal window (Appendix C)

$$\xi_s(R,v) \propto \int_{-\infty}^{\infty} \frac{dv'}{(4\pi\beta)^{1/2}} \exp\left[-\frac{(v-v')^2}{4\beta}\right] \int_{-S}^{S} dz \left(1 - \frac{|z|}{S}\right) \frac{\xi(r)}{D_z(\mathbf{r})^{1/2}} \exp\left[-\frac{v'^2}{2D_z(\mathbf{r})}\right] \quad. \tag{32}$$

The structure function is computed from the formal expression

$$d_s(R,v) = 2\left[\xi_s(0,0) - \xi_s(R,v)\right] \tag{33}$$

where

$$\xi_s(0,0) \propto \int_{-S}^{S} dz \left(1 - \frac{|z|}{S}\right) \frac{\xi(z)}{D_z(z)^{1/2}} \quad, \tag{34}$$

Frequently, the two terms on the right hand side of Eq. (33) are individually divergent, but their combination is not, provided that the subtraction is done before the integration over z.

3.2. *Fluctuations of Density: Correlation Radius r_0*

3.2.1. *Shallow density spectrum*

For shallow density spectra, we use power-law correlation functions of *overdensity*:

$$\xi(r) = \langle\rho\rangle^2 \left(1 + \left[\frac{r_0}{r}\right]^\gamma\right), \qquad \gamma > 0 \tag{35}$$

where r_0 has the physical meaning of the scale at which fluctuations are of the order of the mean density. This ansatz describes properly the situation where the deviations from the mean become uncorrelated at large distances. We have argued in LP04 that the amplitude of density perturbations at the scale of a cloud should not exceed the mean density, which for the shallow density spectrum translates to the requirement that $r_0 < S$.

---

[5] LP00 also contains asymptotics for the regime when shear-like regular motions exceed the turbulent velocities, which can provide a starting point for future detailed consideration of this case.

3.2.2. *Steep density spectrum*

To describe correlations in the random density field with steep (i.e. $n < -3$) power spectrum we start with the structure function given by Eq. (19). Real world structure functions do not grow infinitely and therefore there is a cut-off at some large scale r_c above which the structure function saturates at some limiting value. Being interested in $r \ll r_c$ we shall not address here the issue of the precise form of the saturation and will proceed with a simple ansatz

$$d(r) = d(\infty)\frac{r^{-\gamma}}{r^{-\gamma} + r_c^{-\gamma}} \quad , \quad \gamma < 0 \quad . \tag{36}$$

To find the characteristic correlation length in this case, we note that the correlation function (now well defined because of the cutoff at large scales so that Eq. (21) can be used) is

$$\xi(r) = \frac{1}{2}d(\infty)[1 - d(r)/d(\infty)] + \langle\rho\rangle^2 = \frac{d(\infty)}{2}\frac{r_c^{-\gamma}}{r^{-\gamma} + r_c^{-\gamma}} + \langle\rho\rangle^2 \quad . \tag{37}$$

At sufficiently small $r \ll r_c$ Eq. (37) gives

$$\xi(r) \approx \left(\frac{1}{2}d(\infty) + \langle\rho\rangle^2\right)\left(1 - \frac{d(\infty)}{d(\infty) + 2\langle\rho\rangle^2}[r/r_c]^{-\gamma}\right) \quad . \tag{38}$$

Introducing the correlation scale

$$r_0 = r_c\left[1 + 2\langle\rho\rangle^2/d(\infty)\right]^{-\frac{1}{\gamma}} \tag{39}$$

we recast Eq. (38) in a form similar to Eq. (35)

$$\xi(r) \approx \left(\frac{1}{2}d(\infty) + \langle\rho\rangle^2\right)\left(1 - \left[\frac{r_0}{r}\right]^{\gamma}\right) \quad , \quad \gamma < 0 \tag{40}$$

which allows the uniform treatment of both the steep and shallow cases.

3.2.3. *Physical meaning of r_0*

For a fixed γ the density correlation scale r_0 determines the amplitude of the density fluctuations at a scale r relative to the term that plays the role of the mean uniform density. While for the shallow spectra the uniform density in the volume is just the ensemble average density $\langle\rho\rangle$ (see Eq. (35)), for the steep spectra the role of the uniform density factor is played by $\sqrt{\langle\rho\rangle^2 + d(\infty)/2}$ (see Eq. (40)). The meaning is clear: since the high amplitude density perturbations with the steep spectra are concentrated at the largest scales $\sim r_c$, in a relatively small volume all long-wave modes give mostly uniform offsets of the density, forming a background on which we study small scale ripples. In other words, they serve as local mean densities. The typical magnitude of these modes is described by the dispersion, $\frac{1}{2}d(\infty)$. Besides that, there is a contribution arising from the overall global mean density $\langle\rho\rangle^2$. As the result, $r_0 \geq r_c$ always (see Eq. (39)).

3.3. *Velocity & density: Revisiting LP04*

The term $(1 \pm (r_0/r)^\gamma)$ in the expressions of the density correlation functions given by Eqs. (40) and (35) results in the separation of the of the PPV correlation function into two parts (LP04)

$$\begin{aligned}\tilde{\xi}_s(R, v) &= \tilde{\xi}_v(R, v) + \tilde{\xi}_\rho(R, v),\\ \tilde{d}_s(R, v) &= \tilde{d}_v(R, v) + \tilde{d}_\rho(R, v).\end{aligned} \tag{41}$$

with the v-term describing pure velocity effects, while the ρ-term arises from the actual real space density inhomogeneities that are modified by velocity mapping. To simplify the notation we have dropped the index s from the right-hand-side quantities, since this split is only meaningful in PPV space. This also corresponds to the split in the PPV spectra discussed in LP00.

In LP04 we defined the amplitude of density perturbations for steep spectrum in a different way, which resulted in some confusion, which, fortunately, did not affect our final results there. Here we present a correct discussion of the contribution of the density and velocity fluctuations to the amplitude of fluctuations in PPV.

In PPV space correlation and structure functions are split into two contributions according to Eq. (41), it is possible to see that the term that depends only on velocity fluctuations originates from the effective mean density part in correlation functions (35) and (40), while the ρ-term arises from the density fluctuation part that is modified by velocity fluctuations. The scale r_0 is, thus, critical for establishing their relative magnitudes. Namely, for shallow density spectra (i.e. $\gamma > 0$) the pure velocity effect dominates the density fluctuations at large $r > r_0$, while for the steep density spectra (i.e. $\gamma < 0$) the pure velocity term dominates at small scales, $r < r_0$. Since as we argued in §3.2.3 in the latter case $r_0 > r_c$, the density fluctuations are never dominant for $\gamma < 0$. This discussion invalidates the results in the second column in Table 2 in LP04, where conditions for the dominance of density fluctuations are formulated for $\gamma < 0$. The density term can dominate only if $\gamma > 0$, the regime which is summarized below in the revised Table 1.

In terms of the practical interpretation of observations our present finding allows a more reliable interpretation of the power spectra in terms of underlying velocity fluctuations. Indeed, one should not worry about density contamination of the results of both VCA and VCS if the underlying density spectrum is steep.

Condition	$\gamma > 0$	Eqns
$m \geq \max\left[\frac{2}{3}, \frac{2}{3}(1-\gamma)\right]$	$v^2 < D_z(S)(r_0/S)^m$	(45)-(47)
$\frac{2}{3}(1-\gamma) < m < \frac{2}{3}$	$v^2 < D_z(S)(r_0/S)^{\frac{2/3\gamma m}{m-2/3(1-\gamma)}}$	(45)-(48)
$m \leq \min\left[\frac{2}{3}, \frac{2}{3}(1-\gamma)\right]$	$r_0/S > 1$	(46)-(48)

TABLE 1
Range of the scales where the impact of density inhomogeneities to the PPV statistics exceeds the velocity contribution.

3.4. Asymptotics of line-of-sight PPV correlations

The line-of-sight correlations are of particular importance for our present study. The expression for $\tilde{d}_\rho(0, v)$ is related to the PPV correlation function as

$$\tilde{d}_\rho(0, v) = 2\left[\xi_\rho(0,0) - \xi_\rho(0,v)\right] \quad . \tag{42}$$

A similar expression is valid for $\tilde{d}_v(0, v)$. For the power-law small-scale statistics that we deal with in this paper $\tilde{d}_v(0, v)$ can be obtained from $\tilde{d}_\rho(0, v)$ by setting $\gamma = 0$. Therefore, without losing generality, we shall consider $\tilde{d}_\rho(0, v)$ only, which is given by the integral (see Eqs. (29) and (42))

$$\tilde{d}_\rho(0, v) \sim \left(\frac{r_0}{S}\right)^\gamma \int_{-1}^{1} d\hat{z} \, \frac{1}{|\hat{z}|^{\gamma+m/2}}\left[1 - \exp\left(-\frac{\hat{v}^2}{2|\hat{z}|^m}\right)\right]$$
$$\propto \frac{\bar{\rho}^2 S^2}{D_z(S)} \frac{1}{m}\left(\frac{r_0}{S}\right)^\gamma \left[\frac{1}{p} - \left(\frac{\hat{v}^2}{2}\right)^p \Gamma\left(-p, \frac{\hat{v}^2}{2}\right)\right] \tag{43}$$

where $p = (1-\gamma)/m - 1/2 > 0$ and, to shorten intermediate formulas, the dimensionless quantities $\hat{v} = v/D_z^{1/2}(S)$, $\hat{z} = z/S$, $\hat{r} = r/S$ are introduced. Here Γ is the incomplete gamma-function, but when Γ is used with one argument, the ordinary gamma function is implied.

If we perform the series expansion of the incomplete gamma-function for small argument $\hat{v}$, the square brackets in Eq. (43) provide

$$p^{-1} - 2^{-p}\hat{v}^{2p}\Gamma\left(-p, \hat{v}^2/2\right) = -2^{-p}\hat{v}^{2p}\Gamma[-p] - \left(\frac{1}{2(1-p)}\hat{v}^2 + O(\hat{v}^4)\right) \quad . \tag{44}$$

The informative part of the structure function is in the $\hat{v}^{2p}\Gamma[-p]$ term, while terms in the series part of Eq. (44) individually have no information about the underlying scaling and thus present a problem for a straightforward use of structure functions. For instance, the very first v^2 term in the series is dominant whenever $p > 1$, saturating the structure function at v^2 behavior. [6] More precisely, the leading behavior of the structure function given by Eq. (43) is

$$\tilde{d}_\rho(0, v) \propto \frac{\bar{\rho}^2 S^2}{D_z(S)}\left(\frac{r_0}{S}\right)^\gamma A_{0v}(\gamma, m)\left(\frac{v^2}{D_z(S)}\right)^{\frac{1-\gamma}{m}-\frac{1}{2}} \quad , \quad m > \frac{2}{3}(1-\gamma) \, , \tag{45}$$

$$\tilde{d}_\rho(0, v) \propto \frac{\bar{\rho}^2 S^2}{D_z(S)}\left(\frac{r_0}{S}\right)^\gamma A_{0v}(\gamma, m) \frac{v^2}{D_z(S)} \quad , \quad m < \frac{2}{3}(1-\gamma) \, , \tag{46}$$

with numerical factors $A_{0v}(\gamma, m)$ given in Appendix A. In particular, setting $\gamma = 0$ for the v-term contribution,

$$\tilde{d}_v(0, v) \propto \frac{\bar{\rho}^2 S^2}{D_z(S)} A_{0v}(0, m)\left(\frac{v^2}{D_z(S)}\right)^{\frac{1}{m}-\frac{1}{2}} \quad , \quad m > \frac{2}{3} \, , \tag{47}$$

$$\tilde{d}_v(0, v) \propto \frac{\bar{\rho}^2 S^2}{D_z(S)} A_{0v}(0, m) \frac{v^2}{D_z(S)} \quad , \quad m < \frac{2}{3} \, , \tag{48}$$

Notably, for the pure velocity effect, the value $m = 2/3$, which corresponds to Kolmogorov velocity scaling, presents a boundary case.

Where does the saturation come from? The v^{2p} contribution arises from small spatial separations $z \sim 0$ in the integral in Eq. (43) reflecting small scale turbulent behavior, while v^2 terms come from the longest separations $z \sim S$. Hence, we see that when $p > 1$ the longwave modes of the size of the cloud dominate the velocity structure function even at small velocity separations v and mask the information about the small spatial scales. We therefore have to conclude that the two-point velocity coordinate structure function is not a useful quantity to measure *directly*, unless $m > 2/3(1-\gamma)$, which, in particular, excludes the case when Kolmogorov turbulent velocity dominates the fluctuations of intensity.

However, as we show in §4.1 , the terms that saturate the structure function only provide the contribution to the power spectra that is localized at long wavelengths. Therefore in the Fourier domain one can evaluate the short-wave spectrum of the PPV fluctuations along the velocity coordinate for a more general set of m and γ values.

---

[6] The series expansion for the incomplete gamma-function is irregular at integer p. A rigorous treatment of these cases, most notable of which is the case of Kolmogorov velocity, $m = 2/3, \gamma = 0, p = -1$, gives rise to additional logarithmic factors.

3.5. *Hidden symmetry between line-of-sight and angular PPV correlations*

The Eq. (11) requires the knowledge of $d_s(R, v)$ in both positional, R, and velocity, v, directions. In LP04 we obtained

$$\tilde{d}_\rho(R, 0) \propto -\frac{\bar{\rho}^2 S^2 (r_0/S)^\gamma}{D_z(S)} A_{R0}(\gamma, m) \left(\frac{R}{S}\right)^{1-\gamma-m/2} \tag{49}$$

$A_{R0}(\gamma, m)$ is defined as an integral when the angular dependence of $D_z(\mathbf{r})$ is taken into account (see Appendix A). It reduces to the combination of Gamma functions of LP04 if this dependence is ignored.

Here we want to present a remarkable symmetry between the line-of-sight statistics and the statistics in PP direction. Indeed, the comparison of Eq. (46) and Eq. (49) shows that if one identifies with velocity v a linear scale æ according[7] to

$$v^2 = F(\gamma, m) D_z(S) (æ/S)^m \quad , \tag{50}$$

where $F(\gamma, m) = [A_{R0}(\gamma, m)/A_{0v}(\gamma, m)]^{m/(1-\gamma-m/2)}$, then the line-of-sight structure function $d_s(0, æ)$ acquires the asymptotic form, identical to $d_s(R, 0)$,

$$\tilde{d}_s(0, t) = \tilde{d}_s(t, 0) \propto \left(\frac{t}{S}\right)^{1-\gamma-m/2} \quad . \tag{51}$$

The physical meaning of the new variable æ defined by Eq. (50) is that it defines the scale at which the turbulent velocity dispersion is equal to v. In our turbulent model (see §3.1) we expect that after the transformation Eq. (50), the asymptotic statistics of 3D PPV cubes will be approximately isotropic and the three dimensional PPV distance $r_{\text{PPV}}^2 = R^2 + æ^2$ can be introduced. More exactly, applying the transformation to Eq. (29) for the correlation function
$$d_s(R, æ) = 2 \left(\xi(0, 0) - \xi_s(R, æ)\right)$$

$$\propto \int_{-S}^{S} dz \left[\frac{1}{z^{\gamma+m/2}} - \frac{(R^2 + z^2)^{1-\gamma/2-m/4}}{(1+m/2)R^2 + z^2} \exp\left(-\frac{F(\gamma, m)}{2} \frac{æ^m}{(R^2 + z^2)^{m/2}}\right)\right] \tag{52}$$

and introducing the angle $\cos\theta = æ/r_{\text{PPV}}$, $\sin\theta = R/r_{\text{PPV}}$, we see that the r_{PPV} scaling factorizes

$$d_s(R, æ) \propto (r_{\text{PPV}})^{1-\gamma-m/2} A_{Ræ}(\theta, \gamma, m) \quad , \quad r_{\text{PPV}} \ll S \tag{53}$$

when the integration is extended to infinity, as is appropriate for $r_{\text{PPV}} \ll S$. The integral form for the function $A_{Ræ}(\theta, \gamma, m)$ that describes the angular dependence in $(R, æ)$ space is given in Appendix A. This function is defined so that $A_{Ræ}(\pi/2, \gamma, m) = A_{R0}(\gamma, m)$. With our choice of the coefficient $F(\gamma, m)$ in the transformation relation, $A_{Ræ}(0, \gamma, m) = A_{Ræ}(\pi/2, \gamma, m)$. Figure 1 demonstrates that the variation of $A_{Ræ}(\theta)$ at intermediate angles is typically within ten percent.

In this discussion we have ignored the complication that arises from the saturation of the structure function in the velocity direction. Indeed, the line-of-sight asymptotics of Eq. (45) is valid only for $1 - \gamma - 3m/2 < 0$, a range much narrower than the $1 - \gamma - m/2 < 2$ allowed for Eq. (49). Analysis of this saturation involves taking the limit of the integration in Eq. (52) in the way it is done in Section 3.4.

The issue of the limited validity of structure functions is resolved, if the power spectrum is used directly. For this purpose the spectral formalism of LP00 proves to be useful. In Appendix D we remind the reader of the asymptotic results for the PPV spectrum $P(K, k_v)$ that were obtained in LP00 using a velocity wave number k_v, reciprocal to $v/D_z^{1/2}(S)$. In these variables, the PPV spectrum is manifestly anisotropic, having seemingly very different scalings along and perpendicular to the line-of-sight. The hidden symmetries are revealed if $k_æ \sim 1/æ$ is used.

The symmetry transformation of PPV statistical descriptors allows one to introduce a new technique for determining the turbulent velocity statistics from PPV cubes. Since the mapping Eq. (50) depends explicitly on velocity scaling m and the amplitude of the turbulent motions $D_z(S)$, one can fit for these parameters under the requirement that the structure function or the spectrum of the mapped PPV cube acquire the same scaling in all directions. However this issue is beyond the scope of the present paper. Within this paper the symmetries allow us to generalize our asymptotics obtained for particular PPV directions over a wider PPV volume.

4. VCS FOR A TRANSPARENT MEDIUM: $\alpha \to 0$

The intensity in optically thin lines provides direct information on the density in PPV space. In this case, $\alpha \to 0$, the intensity is given by the linear term in the expansion of the exponent in Eq. (4)

$$I_v(\mathbf{X}) = \epsilon \rho_s(\mathbf{X}, v) \quad . \tag{54}$$

We shall treat separately several limits. First of all, in the limit of high angular resolution (the narrow beam)

$$\mathcal{D}_{nar}(v) \propto \tilde{d}_s(0, v) \tag{55}$$

while in the limit of poor angular resolution (the wide beam) when the spectral data is effectively integrated over the whole image of the object

$$\mathcal{D}_{wide}(v) \propto \int dR R \tilde{d}_s(R, v) \quad . \tag{56}$$

We shall provide a criterion for the transition from one regime to another.

---

[7] We intentionally use a the unusual symbol æ to stress the peculiar non-linear nature of the coordinate transformation that reveals the hidden symmetries in the PPV. Although æ has dimensionality of a distance, one should not confuse it with a real distance to an emitter.

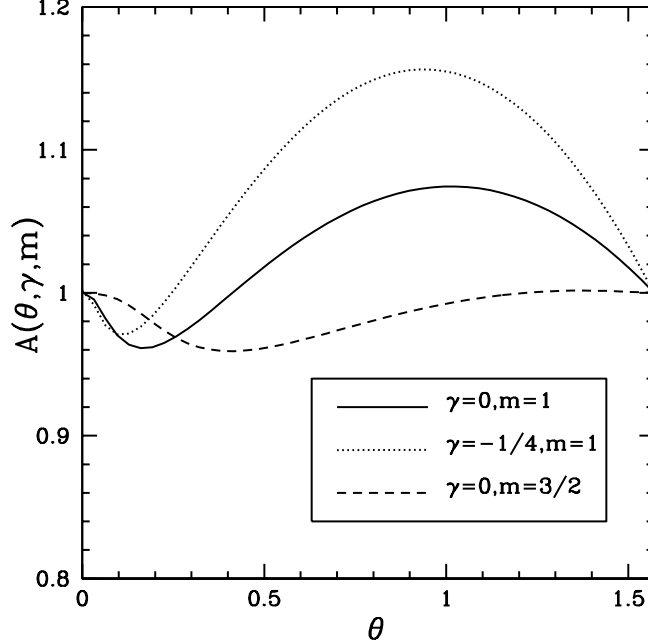FIG. 1.— Function $A_{R\text{æ}}(\theta, \gamma, m)$ for selected γ and m. The variations of the function with the angle θ are moderate, which reflects the hidden symmetry between the PPV variables.

4.1. High Resolution: Narrow Beam

As the first step we consider the case of high resolution. The expressions for $\tilde{d}_s(0, v)$ were discussed in §2.5, where the pitfalls related to the direct use of structure functions along the velocity coordinate were demonstrated. In particular, it was shown that the v^2 contribution arises from the boundary effects. Here we analyze why this contribution is not dominant for the VCS.

The power spectrum is defined for narrow beam studies as

$$P_{nar}(k_v) = -\frac{1}{\sqrt{2\pi}} \int_{-\infty}^{\infty} dv \, \cos[k_v v] \mathcal{D}_{nar}(v). \tag{57}$$

Using Eqs. (43), (55) and (41) we obtain

$$P_{nar}(k_v) \propto e^{-\beta k_v^2} \int_{-1}^{1} d\hat{z} \, |\hat{z}|^{-\gamma} \exp\left[-\frac{1}{2}k_v^2 D_z(S)|\hat{z}|^m\right] \quad, \tag{58}$$

where as before $\hat{z} \equiv z/S$. In the case where the integration over $\hat{z}$ is extended to infinity, we just get

$$P_{nar,inf}(k_v) \propto \frac{2^{\frac{1-\gamma}{m}}}{m} \Gamma\left[\frac{1-\gamma}{m}\right] e^{-\beta k_v^2} \left[k_v D_z^{1/2}(S)\right]^{-2(1-\gamma)/m} \quad, \tag{59}$$

which coincides with the result obtained in the last Appendix of LP00 [8]. There the same result was obtained using the three-dimensional PPV power spectrum $P(\mathbf{K}, k_v)$ in PPV (see Appendix D). Indeed, the narrow-beam $P_{nar}(k_v)$ is given by the integral over $\mathbf{K}$ $P_{nar}(k_v) \propto \int d\mathbf{K} P(\mathbf{K}, k_v)$, thus, $P_{nar}(k_v) \propto P_1(k_v)$, where $P_1(k_v)$ is the one dimensional spectrum defined in LP00.

When the boundary effects are retained

$$P_{nar}(k_v) \propto \frac{2^{\frac{1-\gamma}{m}}}{m} \left(\Gamma\left[\frac{1-\gamma}{m}\right] - \Gamma\left[\frac{1-\gamma}{m}, \frac{k_v D_z^{1/2}(S)}{2}\right]\right) e^{-\beta k_v^2} \left[k_v D_z^{1/2}(S)\right]^{-2(1-\gamma)/m} \quad. \tag{60}$$

Thus, the boundary effects in Fourier space are localized to small k modes, through the incomplete Gamma function term. At high $k_v \to \infty$ this term becomes negligible and we restore the correct power law asymptotics even for very steep slopes $2/m > 3$ (a power spectrum slope of -3 corresponds to a structure function slope -2 in 1D).

---

[8] Direct Fourier transform of the power-law $\mathcal{D}_{nar} = -2^{-p}m^{-1}\Gamma[-p]v^{2p}$ gives, of course, the same result.

4.2. *Poor Resolution: Wide Beam*

The correlations of $I(v)$ are modified when the instrument resolution is poor. In the limit when the turbulent scale (or the whole cloud) is within the beam, we effectively integrate PPV fluctuations over the image, i.e R coordinate. Namely,

$$\mathcal{D}_{wide}(v) \propto \int_0^\infty dR R \tilde{d}_s(R, v) \tag{61}$$

Ignoring the boundary effects and angular dependence of $D_z(\mathbf{r})$ (these do not affect asymptotic scaling) we can join the R and z integrations into a three-dimensional integral to obtain

$$\mathcal{D}_{wide}(v) \propto \frac{\bar{\rho}^2 S^2}{D_z(S)} \int d\hat{r} \, \hat{r}^2 \frac{1}{\hat{r}^{\gamma + m/2}} \left[1 - \exp\left(-\frac{\hat{v}^2}{2\hat{r}^m} \right) \right] \propto \hat{v}^{2\frac{3-\gamma}{m} - 1} \quad , \tag{62}$$

where once more the dimensionless variables $\hat{v} = v/D_z^{1/2}(S)$, $\hat{r} = r/S$ were used. This slope is very steep, e.g., for the pure velocity term, $\gamma = 0$, $6/m - 1 > 2$ for all $m < 2$, and as we have learned in §2.5 the boundary effects saturate the direct structure function measurements at the universal, non-informative[9] slope value 2.

One again we should use the power spectrum which allows the non-informative terms to be weeded out. At high wave numbers k_v the one dimensional VCS in the wide-beam approximation, $P_{wide}(k_v)$, is equal to the three dimensional PPV power spectrum $P(\mathbf{K}, k_v)$ taken at $\mathbf{K} = 0$,

$$P_{wide}(k_v) \propto P(\mathbf{K} = 0, k_v) \quad . \tag{63}$$

Three dimensional PPV power spectrum has been obtained in LP00. We have

$$P_{wide}(k_v) \propto (r_0/S)^\gamma e^{-\beta k_v^2} \left(k_v D_z^{1/2}(S) \right)^{-2(3-\gamma)/m} , \tag{64}$$

where the amplitude of the density contribution is defined through the correlation length r_0. For velocity contribution, $\gamma = 0$,

$$P_{wide}(k_v) \propto e^{-\beta k_v^2} \left(k_v D_z^{1/2}(S) \right)^{-6/m} \tag{65}$$

which provides the high k_v asymptotics for the VCS in the poor resolution regime.

4.3. *Transition from High to Poor Resolution*

A realistic beam has a finite width, ΔB. We remind the reader that we deal with the case in which the emitting volume extend along the line of sight is much smaller than the distance to the volume. As the result, the angular extend of the beam is straightforwardly related to the physical scales that we deal with.

Whether the narrow (Eq. (59)) or wide beam (Eq. (64)) regime is applicable depends on k_v. To the linear scale ΔB corresponds the velocity scale

$$V_{\Delta B} \equiv \sqrt{D(S)(\Delta B/S)^m} \quad , \tag{66}$$

equal to the magnitude of turbulent velocities at the separation of a size ΔB. It is not difficult to find that when

$$k_v^{-1} > V_{\Delta B} \tag{67}$$

the beam is narrow, while on shorter scales its width is important.

The rigorous derivation of this criterion is straightforward. Results in §3.5 and Appendix D allow to describe the VCS as the resolution changes. However, the simplified argument below, that are based on the already derived formulas, gives a more intuitive way to obtaining of the result. Indeed, it is evident, that the difference between the narrow-beam and the wide beam power spectra is the integration over $\mathbf{K}$. One can approximate $P_{nar}(k_v) \propto (\Delta K)^2 P(0, k_v) = (\Delta K)^2 P_{wide}(k_v)$, where ΔK is the size of Fourier domain over which the integral is accumulated. Comparing our results in Eq. (59) and Eq. (64) for the ideally narrow and fully-integrated beams, we find that $\Delta K \sim k_v^{2/m}$. The beam is narrow, if ΔB corresponds to Fourier space integration of at least the size ΔK and is wide otherwise. With proper dimensional coefficients taken into account, we arrive to the criterion in Eq. (67). Another conclusion is that the beam is effectively infinitely wide for all the scales of VCS study, if the beam width exceed the scale at which the underlying structure function of the turbulent velocity saturates (this scale is identified with S in this paper).

4.4. *Expected Regimes for VCS*

In Figure 2 we summarize the different scalings of VCS. As in our earlier papers (LP00, LP04) the main difference stems from the density being either shallow or steep. If the density is shallow i.e. scales as $\xi \sim r^{-\gamma}$, $\gamma > 0$, which means that the correlations increase with the decrease of the scale, then it eventually becomes important at sufficiently small velocity differences, i.e. at sufficiently large k_v. In the opposite case, i.e. when $\gamma < 0$, the contributions of density can be important only at large velocity separations.

---

[9] The situation is a bit better if the density dominates and $\gamma > 0$, but still the parameter range of sensitivity of the structure function remains limited to high $m > 2(1 - \gamma/3)$.

The amplitude of the density contribution to VCS is encoded in the correlation length r_0. The velocity scale that corresponds to r_0 is

$$V_{r_0} = \sqrt{D_z(S)\,(r_0/S)^m} \quad . \tag{68}$$

The comparison of the density (γ is present) and velocity ($\gamma = 0$) contributions to VCS, given by Eq. (59) or Eq. (64) respectively, gives the critical scale when they are equal

$$k_0^{-1} = C(\gamma, m) V_{r_0} \tag{69}$$

The numerical factor $C(\gamma, m) = \sqrt{2}\,(\Gamma[1/m]/\Gamma[(1-\gamma)/m])^{\frac{m}{2\gamma}}$ for a narrow beam and is somewhat different for a wide beam, but in both cases it is of order of unity in the interesting range $-1 < \gamma < 1$ (several aspects of our formalism break down at $\gamma = 1$). So we can roughly equate the scale of equality of the density and velocity effects to r_0, i.e., in velocity units,

$$k_0^{-1} \approx V_{r_0} \quad . \tag{70}$$

The left and middle panels of Figure 2 deal with the case of shallow density. Velocity is dominant at $k_v < k_0$, while the density term provides the main contribution at $k_v > k_0$. The left panel demonstrates the case where the scale of transition from asymptotics is entirely dominated by velocity to the one influenced by spatially resolved velocity and density, $V_{\Delta B} < V_{r_0}$. The observed fluctuations arising from the unresolved turbulent eddies depends on the scalings of both velocity and density. In the middle panel, $V_{\Delta B} > V_{r_0}$, the transition scale is unresolved. In this case if there is still a dynamical range for moderately long scales to be resolved by the experiment $D_z(S)^{1/2} > k_v^{-1} > V_{\Delta B}$, the VCS of the resolved eddies will be determined by the turbulent velocities only.

The right panel of Figure 2 addresses the case of a steep density spectrum. The difference now is that fluctuations of the density are maximal at low wave-numbers and it is there that the density could be important. Velocity is dominant at shorter scales $k_v > k_0$. However, as we discussed in §2.3, the steep density correlation length r_0 is large, at least as large as the density power cutoff r_c, which argues for density fluctuations to be subdominant everywhere up to the scale of the emitting turbulent volume ("cloud"), which is the range of scales that we consider here.
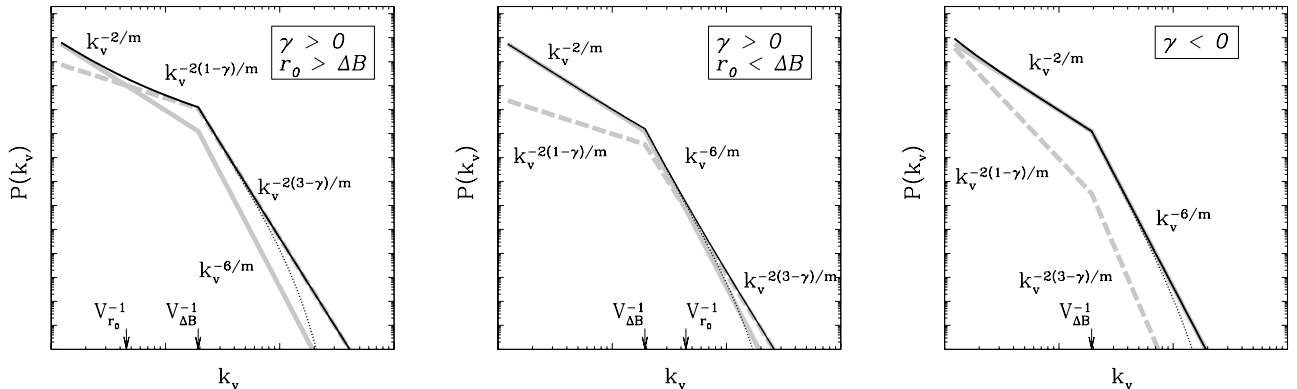

FIG. 2.— Qualitative representation of the density and velocity contributions to the VCS power spectrum and the resulting scaling regimes. In every panel light lines show contributions from the ρ-term (density modified by velocity, dashed line) and v-term (pure velocity effect, solid line) separately, while the dark solid line shows the combined total VCS power spectrum. Thermal suppression of fluctuations is shown by the dotted line. The labels above the dark solid curve are arranged so as to illustrate the sequential transition of the scalings of the total power spectrum. Everywhere except the intermediate regimes, the total spectrum is dominated by one of the components to which the current labeled scaling corresponds. Labels below the dark solid lines mark the scaling of the subdominant contributions. For the left and middle panels the density power spectrum is taken to be shallow, $\gamma > 0$. The left panel corresponds to high amplitude of the density correlations, $r_0 > \Delta B$, where density effects become dominant at relatively long wavelengths for which the beam is narrow. In the middle panel, the amplitude of density correlations is low $r_0 < \Delta B$ and they dominate only the smallest scales which results in the intermediate steepening of the VCS scaling. The right panel corresponds to the steep density spectrum. In this case the density contribution is always subdominant. In this example the thermal scale is five times shorter than the resolution scale $V_{\Delta B}$.

4.5. Thermal Broadening and VCS Cookbook

4.5.1. Thermal effects and inertial range

In Figure 2 we have plotted the power spectra over 3 decades of velocity magnitude to compactly demonstrate all possible scalings. We clearly see two contributions to the VCS, one part arising from pure velocity effects in uniformly distributed matter, while the other represents the contribution of density inhomogeneities modified by the velocity. Thermal effects are shown as well.

In observations, one can anticipate a coverage over two decades of velocity magnitudes before thermal effects get important. Potentially, correcting for the thermal prefactor $\exp(-\beta k_v^2)$ in Eqns. (59,64), one can extend the observational range further. Note, that the thermal corrections are different for species of different mass. Therefore, by using

heavier species one can extend the high k cut-off by the square root of the ratio of the mass of the species to the mass of hydrogen.

How small subsonic (in Cold gas) scales can still be probed depends on the signal-to-noise ratio of the available data. Indeed, the ability to deconvolve the thermal smoothing is limited by noise amplification in the process. However, any extension of the VCS by a factor a in velocity results in the extension of the sampled spatial scales by a factor of $a^{2/m}$, which is a^3 for the Kolmogorov turbulence.

Even with a limited k_v coverage, important results can be obtained with VCS, especially if observations encompass one of the transitional regimes. For example, if one measures a transition from a shallow spectrum to a steeper one (see the left and the right panels in Figure 2) one has the potential to i) determine the velocity index m, since the difference between the slopes is always $4/m$; ii) determine γ next; iii) estimate the amplitude of turbulent velocities from the position of the transition point as discussed above. On the other hand, if one encounters a transition from a steep to a shallower spectrum, one i) may argue for the presence of the shallow density inhomogeneities; ii) estimate γ/m from the difference of the slopes, and then m; iii) estimate the density correlation radius r_0. Finally, if no transition regime is available, as is the case of strong absorption (see Figure 3) than when $\gamma < 0$ one can get m, while for the case of $\gamma > 0$ a combination of γ and m is available.

4.5.2. *Separating thermal and non-thermal velocities*

Consider HI in the Warm and Cold phases as an example. If one disregards, for the sake of simplicity, the cross-correlation between the fluctuations in these two phases, then the VCS from such a system will be a sum of the spectra from $T_{cold} \sim 100$ K and $T_{warm} \sim 10^4$ K gas. It is easy to see that the contribution of the Warm gas to the total VCS may be neglected for all velocities that are subsonic for Warm gas, i.e. for velocities less than 10 km/s. Because the suppression of the Warm gas contribution is exponential, the VCS would reflect the turbulence in the Cold gas, even if the mass fraction of the Cold gas is small. Therefore, to correct for the thermal velocities, one should multiply[10] the VCS power spectrum by $\exp(\beta_{cold}k_v^2)$.

In a more complex model with HI at intermediate temperatures (Heiles & Troland 2003) the cold gas still dominates the VCS. In fact, the machinery that we have developed here allows us to make an independent test of the HI temperatures measured by other techniques. The ability of the VCS to separate of thermal and non-thermal contributions to the line-width makes it a unique tool. One can apply spatial smoothing to the PPV data of a cloud. As the result, the position of the knee between the high and low resolution spectra (see Figure 2) will change. The inverse wavenumber at the knee k_{knee}^{-1} corresponds to the non-thermal velocity at the scale of smoothing θ_{smooth}. Thus we can establish the amplitude of the non-thermal velocities, in particular at the scale of the whole cloud $D_z^{1/2}(S) \approx k_{knee}^{-1}(\theta_{cloud}/\theta_{smooth})^{m/2}$, where m is the index of the velocity structure function that is being determined by the VCS (this index is $m = 2/3$ for Kolmogorov turbulence) and θ's are angular sizes of the cloud and the smoothing length. This allows one to measure cloud gas temperatures. We shall discuss the details of this technique elsewhere. Choosing the correct factor of $\exp(\beta_{cold}k_v^2)$ to straighten the VCS plot can be another procedure for determining the cold gas temperature (e.g. Chepurnov & Lazarian 2006).

4.5.3. *VCS cookbook*

The VCS cookbook is rather straightforward. VCS near a scale k_v depends on whether the instrument resolves the correspondent spatial scale $\left[k_v^2 D_z(S)\right]^{-1/m} S$, where S is the scale where turbulence saturates. If this scale is resolved then $P_v(k_v) \propto k_v^{-2/m}$ and $P_\rho(k_v) \propto k_v^{-2(1-\gamma)/m}$. If the scale is not resolved then $P_v(k_v) \propto k_v^{-6/m}$ and $P_\rho(k_v) \propto k_v^{-2(3-\gamma)/m}$. These results are presented in a compact form in Table 2. The transition from the low to the

Spectral term	$\Delta B < S \left[k_v^2 D_z(S)\right]^{-\frac{1}{m}}$	$\Delta B > S \left[k_v^2 D_z(S)\right]^{-\frac{1}{m}}$
$P_\rho(k_v)$	$\propto \left(k_v D_z^{1/2}(S)\right)^{-2(1-\gamma)/m}$	$\propto \left(k_v D_z^{1/2}(S)\right)^{-2(3-\gamma)/m}$
$P_v(k_v)$	$\propto \left(k_v D_z^{1/2}(S)\right)^{-2/m}$	$\propto \left(k_v D_z^{1/2}(S)\right)^{-6/m}$

TABLE 2
SCALINGS OF VCS FOR SHALLOW AND STEEP DENSITIES.

high resolution regimes happens as the velocity scale under study gets comparable to the turbulent velocity at the minimal spatially resolved scale. As the change of slope is the velocity-induced effect, it is not surprising that the difference in spectral indexes in the low and high resolution limit is $4/m$ for both P_v and P_ρ terms, i.e it does not depend on the density[11]. This allows for separation of the velocity and density contributions. For instance, Figure 2

---

[10] In a similar way one can treat the velocity resolution of the instrument. However, in this case, similar to the case of the thermal broadening corrections, the extent to which the VCS can be extended is limited by the noise amplification that the procedure entails.

[11] In the situation where the available telescope resolution is not sufficient, i.e. in the case of extragalactic turbulence research, the high spatial resolution VCS can be obtained via studies of the absorption lines from point sources.

illustrates that in the case of shallow density both the density and velocity spectra can be obtained.

Note that obtaining the density spectrum from a well resolved map of intensities is trivial for the optically thin medium, as the density spectrum is directly available from the column densities (i.e. velocity integrated intensities). However, for the absorbing medium such velocity-integrated maps provide the universal spectrum K^{-3}, where K is the 2D wavenumber (LP04). Similarly, even for the optically thin medium, it is not possible to get the density spectrum if the turbulent volume is not spatially resolved. On the contrary, $P_\rho(k_v)$ reflects the contribution of shallow density even in this case (see Figure 2).

5. EFFECTS OF ABSORPTION

The main *scale dependent* effect of absorption is to diminish correlation between intensity of emission at widely separated velocities or lines of sight, i.e from distant points in PPV space. The effect of absorption has been discussed at length in LP04 in the framework of the VCA technique. Here we capitalize on the insight obtained there.

Along the velocity coordinate the separations that are affected by absorption can be estimated using Eq (16). Similar to LP04 we get that the absorption becomes important when $\alpha^2 d_s(0, v) > 1$, thus for v exceeding the absorption velocity scale V_{ab} which we define as

$$\alpha^2 \tilde{d}_s(0, V_{ab}) = 1 \qquad . \tag{71}$$

Let us consider in detail the $\gamma < 0$ case when the velocity term dominates VCS. Asymptotic expressions for d_v given by Eq. (47) and (48) lead to the absorption window width

$$V_{ab}/D_z(S)^{1/2} \approx (\alpha\bar{\rho}_s)^{\frac{2m}{m-2(1-\gamma)}}, \qquad m > 2/3 \tag{72}$$

$$V_{ab}/D_z(S)^{1/2} \approx (\alpha\bar{\rho}_s)^{-1} \qquad , \qquad m < 2/3 \tag{73}$$

where we have omitted numerical coefficients of order unity and have estimated $\bar{\rho}_s = \bar{\rho}S/D_z(S)^{1/2}$.

For our purpose of studying turbulence over its power-law inertial range, the only velocity range that matters is $v < V_{ab}$.

When the resolution of the instrument is finite and signal is averaged over an angular area, absorption determines how distant lines-of-sight contribute to the correlated signal. This effect is described by the absorption window $W_{ab}(R)$, introduced in §2 (see Eq. (13)), which behaves similar to the instrument beam, downweighting the distant pairs.

Let us estimate the form of the window assuming Gaussian statistics and homogeneity of the density fluctuations $\delta\rho_s = \rho_s - \langle\rho_s\rangle$. Then (see LP04)

$$W_{absorption} \approx \langle e^{-\alpha\rho_s(\mathbf{X_1},v_1)}\rangle \langle e^{-\alpha\rho_s(\mathbf{X_2},v_1)}\rangle e^{\frac{\alpha^2}{2}\langle\delta\rho_s^2(\mathbf{X_1},v_1)+\delta\rho_s^2(\mathbf{X_2},v_1)\rangle} e^{-\frac{\alpha^2}{2}\tilde{d}_s(R,0)} \tag{74}$$

The last term is the one that determines the scale dependence of the window. The most important qualitative characteristic of the window is its width, which for absorption we shall define as R_{ab} at which

$$\alpha^2 \tilde{d}_s(R_{ab}, 0) = 1 \qquad . \tag{75}$$

In terms of the velocity-density decomposition of the PPV structure function, the product of the two windows arises, which is $\sim e^{-\alpha^2\tilde{d}_v(R,0)/2}e^{-\alpha^2\tilde{d}_\rho(R,0)/2}$. Both factors act simultaneously but the one with the smallest width determines the gross effect. This is $d_v(R,0)$ for $\gamma < 0$. Setting $\gamma = 0$ in Eq. (49) to obtain the asymptotics for $d_v(R,0)$ we get

$$R_{ab}/S \approx (\alpha\bar{\rho}_s)^{\frac{2}{m-2}} \qquad . \tag{76}$$

One must compare the absorption window scale R_{ab} to the beam ΔB on one hand, and to the scales under study v on the other hand. When $R_{ab} > \Delta B$, the absorption window is not important. In the opposite regime, $R_{ab} < \Delta B$, when the absorption affects the angle averaging, one compares the velocity scale, corresponding to R_{ab}, $V_{ab} = D_z^{1/2}(S)(R_{ab}/S)^{m/2}$, with v. For $v < V_{ab}$ the effective window is a low resolution one, while for $v > V_{ab}$ absorption seems to induce an effective high resolution beam. Given the symmetry between the line-of-sight and orthogonal sky correlations that we discussed in §3.5, it is, however, no surprise that V_{ab} defined this way coincides with the critical velocity separation given by Eq. (73) above which absorption destroys the power-law scaling solutions. Hence, one cannot recover the high resolution scaling laws with the help of absorption effects.

Thus, we conclude that to study the inertial turbulence range one should focus on $v < V_{ab}$ and to be able to measure high-resolution asymptotic VCS one must have instrument resolution better than the 'absorption window, $V_{\Delta B} < V_{ab}$ (see Figure 3).

6. DISCUSSION

6.1. *Simplifications Employed*

To simplify our presentation we considered emission that is proportional to the first power of density. However, we found that for many cases, e.g. for steep density, the actual spectrum of density is irrelevant. Therefore these results are not affected by the actual assumptions about the scaling of emissivity. In general, our results may be trivially generalized if correlation functions of emissivities are used instead of correlation functions of densities (Chepurnov & Lazarian 2006). With this in mind we may claim that the VCS is applicable not only to HI, but also to CO transitions, emission by ions in turbulent plasmas, various molecules etc.
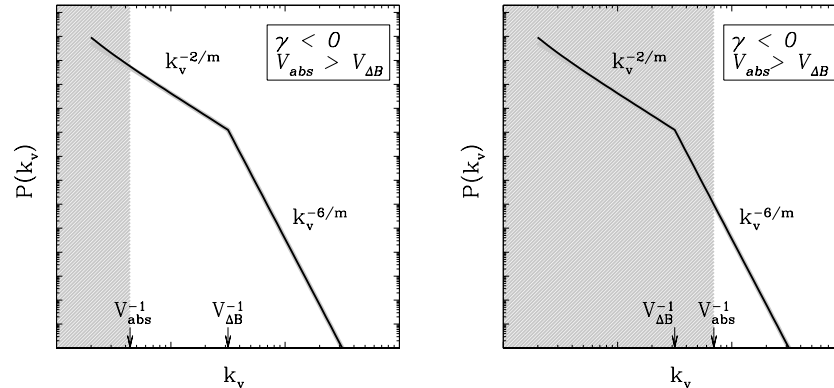
Fig. 3.— Qualitative representation of the absorption effects on the VCS power spectrum and the resulting scaling regimes. Shaded region corresponds to the regimes obscured in the presence of absorption.

Following LP04 in the paper we employed a simplified treatment of the radiative transfer. However, it is explained in LP04 that a more elaborate treatment of absorption cannot change the high wavenumber asymptotics that we are interested in. In short, at low k_v the absorption gets important and it destroys the power-law behavior. We do not have predictions for the VCS in this regime. However, our results show that at sufficiently high k_v (which depends on the window function determined by the absorption) the power-laws are not affected and the VCS can be used to study turbulence.

Note, that in the paper above we have analyzed the problems of using structure functions along the velocity coordinate being very steep. One possible way of proceeding with a real space statistical description in this case is to design a 'next order' structure function which will have a counter-term eliminating the contaminating quadratic in velocity term. Such 'next order' function will be insensitive not only to the constants added to the field, but also to the gradients of the field. We shall not develop higher order structure function formalism here. (Eq. (44) gives a good guidance on what terms need to be canceled). Instead, we argue for using spectra along the velocity coordinate which allows us to avoid a lot of unnecessary trouble.

6.2. VCS and Other Techniques

6.2.1. VCS & VCA: optically thin lines

A unique feature of the VCS is that this technique utilizes information that has not been used before, as far as we know. Indeed, we developed the VCA in LP00 to explain the puzzling data on spectra of PPV slices (see Green 1993). The motivation for LP04 was both to study the domain of applicability of VCA in the presence of absorption and to explain the CO line integrated data (see Stutzki et al. 1998). The situation is different with the VCS, where the practical application of the technique to the actual data has just started (see Lazarian 2004, 2005, 2006, Chepurnov & Lazarian 2006).

The earlier techniques to study turbulence, e.g. velocity centroids or VCA require the observations to spatially resolve the scale of the turbulence under study[12]. This constrains the variety of astrophysical objects where the turbulence can be studied. The technique presented here, namely, the VCS, is a unique tool that allows studies of astrophysical turbulence even when the instrument does not resolve the turbulent fluctuations spatially. Indeed, it is essential for the technique to resolve only the fluctuations of intensity along the V-axis (see §4.2). This is of immense importance for studies of turbulence in poorly resolved extragalactic objects, supernova remnants and circumstellar regions[13]. There is also potential for the modification of the technique for laboratory research, e.g. for plasma turbulence studies.

Our study of the effect of finite temperatures for the technique reveals that, unlike the VCA, the temperature broadening does not prevent the turbulence spectrum from being recovered from observations. Indeed, in VCA, gas temperature acts in the same way as the width of a channel. Within the VCS the term with temperature gets factorized. One can correct for this term, e.g. by fitting for the temperature that would remove the exponential fall off in the spectrum. This also allows for a new way of estimating the interstellar gas temperature (see Chepurnov & Lazarian 2006).

Another advantage of the VCS compared to the VCA is that it reveals the spectrum of turbulence directly, while within the VCA the slope of the spectrum should be inferred from varying the thickness of the channel. As the thermal line width acts in a similar way as the channel thickness, additional care (see LP04) should be exercised not

[12] As it was discussed in LP00, the VCA can be applied directly to the raw interferometric data, rather than to images that require good coverage of all spatial frequencies. However, even with interferometers, the application of the VCA to extragalactic objects is restricted.

[13] For some of these objects the issue of isotropy and homogeneity of turbulence may arise. Indeed, if the properties of turbulence change substantially along the line of sight, the measured spectra would represent the averaged properties of turbulence. To get more detailed information one may need to average the fluctuation arising, for instance, from a supernova remnant, over annuli over the image, which would require some spatial resolution, but may not still require resolving the spatial turbulent scale under study.

to confuse the channel that is still thick due to thermal velocity broadening with the channel that shows the thin slice asymptotics. We feel that a simultaneous use of VCA and the VCS makes the turbulence spectrum identification more reliable.

6.2.2. *VCS & VCA: self-absorption and absorption lines*

The introduction of absorption in VCS and VCA brings about different results. Within the analysis of velocity slices spectra (VCA) the absorption results in new scalings for slices for which absorption is important. The turbulence spectral indexes can be recovered for the VCA within sufficiently thin slices, provided that the thickness of the slices exceeds the thermal line width. For the VCS no new power-law asymptotics is available in the presence of absorption. When absorption becomes important the spectra get exponentially damped. This simplifies the interpretation of the data.

As we discussed in LP00 and LP04 the VCA is applicable to studies of not only emission, but also absorption lines. An example of such a study is provided in Deshpande, Dwarakanath & Goss (2000), where an extended synchrotron emission background was used to map the absorption in the HI gas. The necessity of using extended emission sources limits the extent of possible VCA studies of turbulence. This is not an issue for the VCS, for which absorption lines[14] from *point sources* can be used. Interestingly enough, in this case the VCS asymptotics for the high resolution limit should be used irrespectively of the actual beam size of the instrument.

6.2.3. *Relation to other techniques*

Talking about the role of the present study in a more general framework of the techniques for studies of turbulent velocities we would say that this paper provides a formalism that should allow to describe the properties of Spectral Correlation Functions (SCF) (see Padoan, Goodman & Juvela 2003 and references therein) in the presence of absorption. The relation, however, between these techniques and another statistical tool, namely, Principal Component Analysis (PCA) (see Heyer & Brunt 2004 and references therein) is not yet clear.

Taking turbulence studies in a broader context, we may note, that similar to the successful studies of electron density fluctuations in the ionized media (see Spangler & Gwinn 1990) the VCS can study turbulence without requiring high spectral resolution. Note, however, that the aforementioned scintillation studies have limitations arising from limited number of sampling directions as well as from the technique being relevant only for ionized gas at extremely small scales. Moreover, these sorts of measurements provide only the density statistics, which is an indirect measure of turbulence. Naturally, combining information on turbulence obtained by different channels provides big advantages for constraining the models of interstellar turbulence and testing its correspondence with the theoretical expectations[15].

6.3. *Progress and Prospects*

While establishing the mathematical foundations of the VCS, in this paper we have improved the statistical description of the PPV. In particular, we established the source of problems related to the use of structure functions along the velocity coordinate and proposed a remedy. In addition, we corrected our earlier statements about the relative importance of density and velocity contribution in the case when the density is steep. As the result, we established that the for a steep density spectrum, the density contribution is always subdominant. This fact simplifies practical studies of turbulence both using the VCS and the VCA.

We have extended the general theory of the correlations in PPV space. Potentially, although we did not pursue this within this paper, our findings on the symmetries existing in the PPV space open a way to study the velocity field using the entire PPV data cubes, rather than slices, as we use in the VCA, or along-the-line statistics as we use in the VCS. This also allows one to extend the centroids and modified centroids (Lazarian & Esquivel 2003, Esquivel & Lazarian 2005) techniques for studies of turbulence in the presence of absorption.

In §4.5 we have discussed the thermal broadening using HI as an example. Using heavier species that exhibit lower thermal broadening allows one to study turbulence up to smaller scales. One can extend the range of environments that can be proved by the VCS using different wavelengths. For instance, the X-ray spectrometers with high spatial resolution can be used to study of turbulence in hot plasma. In particular, the potential of VCS is high for studies of plasma turbulence in clusters of galaxies (see Sunyaev et al. 2003 and references therein). A simulated example of such a study with the future mission Constellation X is provided in Lazarian (2006).

Studies of turbulence in objects which are poorly resolved spatially is a natural avenue for the VCS applications. Interestingly enough, in this case one can combine the absorption line studies, which would provide the VCS for the

---

[14] The mathematical formulation to the problem of the VCS for absorption lines are very similar to the VCS for emission lines. The absorption for optical and UV lines for which stimulated emission is negligible is proportional to $\int_0^S dz\rho(\mathbf{x})\phi_v(\mathbf{x})$ and therefore measurements of the absorbed intensity can be treated the same way as the intensity of the emission spectral line in §2.1. The difference is that this case is simpler as one should not worry either of the finite resolution or absorption effects. In the case of HI absorption study of the ratio of density over temperature enters instead of density. In the case of an isobaric medium the product of density and temperature are constant and the problem is similar to studies of transitions for which the emissivity is proportional to ρ^2. In general, our study shows that the VCS in most cases is dominated by velocity fluctuations. Thus we expect that the temperatures should not much affect the VCS even for HI absorption line studies.

[15] For instance, the issues of whether the Alfvenic turbulence has Kolmogorov spectrum of $-5/3$ or the Iroshnikov-Kraichnan spectrum of $-3/2$ have been widely discussed in the literature (e.g. Maron & Goldreich 2001, Muller, Biskamp & Grappin 2003, Biskamp 2003, Boldyrev 2005, Beresnyak & Lazarian 2006). The difference in the VCS slopes for these two underlying spectra is 1, which can be found through observations. Defining the type of spectrum is important for many applications, including thermal conduction, cosmic ray and cosmic dust dynamics (see Lazarian 2006ab, Cho & Lazarian 2006, Yan, Lazarian & Draine 2004 and references therein.

high resolution, with the emission studies that would provide the VCS in the poor resolution limit. Potentially, both velocity and density spectra can be obtained this way.

The importance of this work goes beyond the actual recovery of the particular power-law indexes. First of all, the technique can be generalized to solve the inverse problem to recover non-power law turbulence spectra. This may be important for studying turbulence at scales at which either injection or dissipation of energy happens[16]. Such studies are important for identifying astrophysical sources and sinks of turbulent energy. Second, studies of the transition from low resolution to high resolution regimes allows one to separate thermal and non-thermal contributions to the line-widths as has been discussed in §4.4. This could both test the thermal correction that can be applied to extend the power-law into sub-thermal velocity range (see §4.4 and Chepurnov & Lazarian, 2006) and enable studies of temperature distribution of the gas in atomic clouds (Heiles & Troland, 2003).

7. SUMMARY

I. VCS is a new technique to study astrophysical turbulence in interstellar gas, intracluster plasma, supernova remnants etc. Its major advantage to the existing techniques is that it does not necessarily require high spatial resolution to recover the information on turbulence.

II. VCS can employ both absorption and emission lines to study turbulence. The current study concentrates mostly on emission lines and develops a mathematical formalism that may be modified to deal with absorption lines. We account for the effects of thermal broadening and self-absorption.

III. VCS has two parts, one depending exclusively on velocity and the other depending on both velocity and density: the relative amplitude of the two terms depends on the amplitude of density perturbations and the dominance of the particular part depends on whether density statistics is shallow or steep:

a) if the density statistics is steep ($P(k) \propto k^{-n}, n > 3$), the VCS is affected only by the turbulent velocity.

b) if the density spectrum is shallow, then at small wave-numbers the VCS is affected only by the velocity fluctuations and at larger wave-numbers - by both density and velocity fluctuations. The wavenumber corresponding to the transition point between the two regimes above depends on the amplitude of the density fluctuations.

IV. The particular power-law indexes of the VCS depend on whether the fluctuations under study are spatially resolved or not. The transition from one regime to another occurs for velocities corresponding to the minimal spatially resolved scale. The density and velocity contributions can be separated by smoothing the data. The difference between the VCS spectral indexes for low resolution and high resolution depends only on the spectrum of the velocity fluctuations.

V. The transition between the low and high resolution regimes allows one to identify the spatial scale associated with a particular turbulent velocity. Therefore observing this transition provides a way to relate the velocity dispersion with the angular separation between the lines of sight. This allows one to separate thermal and nonthermal contribution to line broadening in clouds.

VI. VCS allows the recovery of the underlying spectrum of turbulence in the presence of absorption. For the power-law spectra, the main effect of absorption amounts to the introduction of the low frequency spatial filter for the fluctuations along the velocity coordinate.

VII. Both in cases of negligible and important absorption thermal broadening of spectral lines introduces the exponential suppression of the amplitude of the high frequency VCS, which makes cold gas the most important contributor to the VCS signal. This suppression is factorized in the expressions for the VCS and it can be corrected for by choosing the particular exponential factor that straightens the VCS to a power law at large k_V. Choosing this correction provides yet another way of estimating the temperature of cold gas.

---

[16] Consider turbulent damping scale. The study can provide us with the angular scale at which damping occurs, i.e. with the ratio of d_{diss}/L, where L is the distance to the cloud under study. Thus if we know the distance, we can have an insight into the damping of turbulence and therefore the physical conditions in the cloud. Alternatively, there are situations where the distance to the cloud is notoriously poorly known, as this is the case of high velocity clouds (see Wakker 2004). In such situations the calculations of d_{diss} scale (see expressions (20) and (6) in Lazarian et al. (2004), where d_{diss} should be identified with the inverse of the critical perpendicular wavenumber) can be provided with higher accuracy using the velocity dispersion at the scale of the cloud. This allows to place better limits on L.

for Magnetic Self Organization in Laboratory and Astrophysical Plasmas.

APPENDIX

A. NOTATIONS

$\rho(\mathbf{x})$	3D density field.
$\mathbf{u}(\mathbf{x})$	3D turbulent velocity field.
$\xi(r)$	3D density correlation function.
$\mathrm{d}(r)$	3D density structure function.
$D_z(r)$	z-component of 3D velocity structure function.
$\rho_s(\mathbf{X}_1, v_1)$	density in PPV space .
$\xi_s(R, v)$	PPV density correlation function.
$\mathrm{d}_s(R, v)$	PPV density structure function.
$\tilde{\xi}_s(R, v)$	PPV density fluctuations correlation function.
$\tilde{\mathrm{d}}_s(R, v)$	PPV density fluctuations structure function.
$I(\mathbf{X}_1, v_1)$	emission intensity at velocity v_1 in the direction $\mathbf{X}_1$.
$\mathcal{D}(v_1, v_2)$	intensity structure function along the velocity coordinate.
$P(k_v)$	power spectrum of intensity along the velocity coordinate.
æ	coordinate in velocity direction rescaled to reveal P-V symmetries
$B(\mathbf{X})$	angular beam of the instrument.
S	saturation scale of the turbulent velocities. Identified with the spatial extend of the turbulent cloud.
$D_z^{1/2}(S)$	characteristic turbulent velocity difference at separation S. Sets the extend of the spectral line along the velocity coordinate.

$$A_{0v}(\gamma, m) = \begin{cases} 2^{\frac{3}{2} - \frac{1-\gamma}{m}} \Gamma\left(\frac{3}{2} - \frac{1-\gamma}{m}\right)/(1 - \gamma - m/2), & m > \frac{2}{3}(1-\gamma) \\ 1/(1 - \gamma - 3m/2), & m \leq \frac{2}{3}(1-\gamma) \end{cases}.$$

$$A_{R0}(\gamma, m) = 2 \int_0^\infty dz \left[z^{-\gamma - m/2} - (1+z^2)^{1-\gamma/2 - m/4}/(1 + m/2 + z^2)\right].$$

$$A_{R\text{æ}}(\theta, \gamma, m) = 2 \int_0^\infty dz \left[z^{-\gamma - m/2} - \frac{(\sin^2\theta + z^2)^{1-\gamma/2 + m/4}}{(1+m/2)\sin^2\theta + z^2} \exp\left(-\frac{A(\gamma, m)}{2} \frac{\cos^m\theta(\sin^2\theta + z^2)^{1-m/2}}{(1+m/2)\sin^2\theta + z^2}\right)\right].$$

$$F(\gamma, m) = [A_{R0}(\gamma, m)/A_{0v}(\gamma, m)]^{m/(1-\gamma - m/2)}.$$

$$C(\gamma, m) = \sqrt{2}\left[\Gamma(1/m)/\Gamma((1-\gamma)/m)\right]^{m/2\gamma}.$$

B. HOMOGENEITY OF DATA AND REDUCTION OF NOISE

For practical data handling one has to deal with the actual line shape. An important issue is whether the statistics along the V-coordinate can be assumed homogeneous, in which case the statistical descriptors are the functions of the velocity separation $v = v_1 - v_2$ only, $\mathcal{D}(v_1, v_2) = \mathcal{D}(v)$. To be valid this requires statistical homogeneity of the PPV density, which, in particular, corresponds to the case of a flat mean line profile $\langle I_{\mathbf{X}}(v) \rangle = const$ for the velocities under consideration. More generally, one would like to subtract the mean line profile, and assume homogeneity for the fluctuations only.

Whether statistics is homogeneous or not is also important to our ability to measure it with the noisy data. In the measurements, the ensemble average $\langle \ldots \rangle$ is replaced by the volume average over the space in which the statistics is homogeneous, i.e. does not change with the translations in space. Take $\mathcal{D}(v_1, v_2)$. How can we estimate it from the data ? If it depends separately on v_1 and v_2 and we have only a single line of sight, then there is no averaging available and our estimate of the correlation will be very noisy $\mathcal{D}(v_1, v_2) \approx [I(v_1) - I(v_2)]^2$. For homogeneous statistics, however, we can average over $v_+ = (v_1 + v_2)/2$, $\mathcal{D}(v) \propto \int dv_+ [I(v_1) - I(v_2)]^2$, beating the noise down significantly. However, if we have measurements at several lines of sight, we can average our estimator over $\mathbf{X}$ which may give us the ability to measure even inhomogeneous $\mathcal{D}(v_1, v_2)$.

Statistics of the fluctuations will then be described by the modified structure function

$$\tilde{\mathcal{D}}(v) = \langle [I(v_1) - \langle I(v_1) \rangle] [I(v_2) - \langle I(v_2) \rangle] \rangle = \mathcal{D}(v_1, v_2) - [\langle I(v_1) \rangle - \langle I(v_2) \rangle]^2 \tag{B1}$$

Eq. (B1) indicates that at small separations v the correction due to the mean profile is at least quadratic in v, $[\langle I(v_1) \rangle - \langle I(v_2) \rangle]^2 \sim v^2$. As we discuss in §2.5 this results in an easily separable δ function contribution to the VCS.

C. STATISTICS OF DENSITY IN PPV

The random fields $\rho(\mathbf{x})$ and $u(\mathbf{x})$ are assumed to be uncorrelated. The accuracy of this assumption was studied analytically in LP00, LP04 and tested numerically in Lazarian et al. (2001), and Esquivel et al. (2003). As the result, this key assumption was shown to be accurate both for the data obtained via MHD turbulence simulations as well as for particular general type flows that were treated analytically. We shall also consider statistical properties of the density distribution $\rho(\mathbf{x})$ to be homogeneous.

Under these assumptions, the mean and the two-point correlation function of the PPV density are given, corre-

spondingly, by

$$\langle \rho_s(\mathbf{X}_1, v_1) \rangle = \int_0^S dz_1 \, \langle \rho(\mathbf{x}_1) \rangle \langle \phi_{v1}(\mathbf{x}_1) \rangle =$$

$$= \bar{\rho} \int_0^S dz_1 \, \langle \phi_{v1}(\mathbf{x}_1) \rangle \quad , \tag{C1}$$

$$\langle \rho_s(\mathbf{X}_1, v_1)\rho_s(\mathbf{X}_2, v_2) \rangle = \int_0^S dz_1 \int_0^S dz_2 \, \langle \rho(\mathbf{x}_1)\rho(\mathbf{x}_2) \rangle \, \langle \phi_{v1}(\mathbf{x}_1)\phi_{v2}(\mathbf{x}_2) \rangle =$$

$$= \int_0^S dz_1 \int_0^S dz_2 \, \xi(\mathbf{r}) \langle \phi_{v1}(\mathbf{x}_1)\phi_{v2}(\mathbf{x}_2) \rangle \quad . \tag{C2}$$

The computation is, thus, reduced to evaluating the ensemble average of the products of the Maxwell functionals $\phi_v(\mathbf{x})$ over the Gaussian distribution of the turbulent velocities u, i.e, $\langle \phi_{v1}(\mathbf{x}_1) \rangle = \int du_1 \phi_{v1}(\mathbf{x}_1)P(u_1)$ and $\langle \phi_{v1}(\mathbf{x}_1)\phi_{v2}(\mathbf{x}_2) \rangle = \int du_1 du_2 \phi_{v1}(\mathbf{x}_1)\phi_{v2}(\mathbf{x}_2)P(u_1, u_2)$, $u_1 = u(\mathbf{x}_1)$, $u_2 = u(\mathbf{x}_2)$. In our picture we identify the scale S at which the structure function $D_z(\mathbf{r})$ that describes the turbulent field is saturated $D_z(\infty) \approx D_z(S)$ with the size of the emitting cloud. The one point distribution function of the line-of-sight velocity component is then

$$P(u_1) = \frac{1}{\sqrt{\pi D_z(S)}} \exp\left[-\frac{u_1^2}{D_z(S)}\right] \tag{C3}$$

(the velocity is defined with respect to the rest frame of the cloud, and is, thus, taken to have a zero mean) while the Gaussian two point probability function is most conveniently given in terms of the uncorrelated variables $u = u_1 - u_2$ and $u_+ = (u_1 + u_2)/2$

$$P(u, u_+) = \frac{1}{\pi\sqrt{2D_z(S) - D_z(\mathbf{r})}\sqrt{D_z(\mathbf{r})}} \exp\left[-\frac{u_+^2}{D_z(S) - D_z(\mathbf{r})/2}\right] \exp\left[-\frac{u^2}{2D_z(\mathbf{r})}\right] \tag{C4}$$

In LP04 we obtained the general results. Here we reproduce the results of the computation just for the case of vanishing regular shear velocities v_{gal} that are dealt with in this paper

$$\langle \rho_s(\mathbf{X}_1, v_1) \rangle = \frac{\bar{\rho}S}{\sqrt{\pi}\,[D_z(S) + 2\beta]^{1/2}} \exp\left[-\frac{v_1^2}{D_z(S) + 2\beta}\right] \tag{C5}$$

$$\langle \rho_s(\mathbf{X}_1, v_1)\rho_s(\mathbf{X}_2, v_2) \rangle = \frac{1}{2\pi} \int_{-S}^S dz \,(S - |z|) \, \frac{\xi(\mathbf{r})}{[D_z(\mathbf{r}) + 2\beta]^{1/2}} \exp\left[-\frac{v^2}{2(D_z(\mathbf{r}) + 2\beta)}\right]$$

$$\times \frac{\sqrt{2}}{[\beta + D_z(S) - D_z(\mathbf{r})/2]^{1/2}} \exp\left[-\frac{v_+^2}{\beta + D_z(S) - D_z(\mathbf{r})/2}\right] \quad , \tag{C6}$$

where we used the notation $v = v_1 - v_2$, $v_+ = (v_1 + v_2)/2$, $\mathbf{r} = \mathbf{r}_1 - \mathbf{r}_2$, $z = z_1 - z_2$, $\mathbf{R} = \mathbf{X}_1 - \mathbf{X}_2$.

The residual dependence of the quantities in Eqs. (C5-C6) on the absolute velocity v_1 or v_+ is the signature of statistical inhomogeneity of the density in PPV space at the edges of the line $|v_1|, |v_+| > (D_z(S) + \beta)^{1/2}$. However, we are interested primarily in the $\mathbf{X}$ and v dependence of PPV correlations at separations small compared with the extent of the cloud in PPV space. If the measurements are done in a narrow velocity channel, then the inhomogeneity means a different normalization of the correlation function for channels at the edge of the line relative to central channels. If localization along the velocity coordinates is not focused upon, the observed correlations can, and often are, estimated by averaging over all central velocities v_+ for the fixed v. Whenever the observed signal is linearly related to the density in PPV, as in the case of the intensity in an optically thin line, such estimation is given by the PPV density correlation averaged along the velocity coordinate

$$\xi_s(\mathbf{R}, v) \approx \frac{1}{[D_z(S) + 2\beta]^{1/2}} \int dv_+ \langle \rho_s(\mathbf{X}_1, v_1)\rho_s(\mathbf{X}_2, v_2) \rangle \tag{C7}$$

$$\approx \frac{\bar{\rho}^2 S}{[D_z(S) + 2\beta]^{1/2}} \int_{-S}^S dz \left(1 - \frac{|z|}{S}\right) \frac{\xi(\mathbf{r})/\bar{\rho}^2}{[D_z(\mathbf{r}) + 2\beta]^{1/2}} \exp\left[-\frac{v^2}{2(D_z(\mathbf{r}) + 2\beta)}\right]$$

which is not sensitive to the mean line profile. In this paper we shall not consider scales comparable to the whole extent of the line and will use Eq. (C7) as our main formula for $v \ll D_z^{1/2}(S)$.

At vanishing temperature

$$\xi_s(\mathbf{R}, v) \approx \frac{\bar{\rho}^2 S}{D_z^{1/2}(S)} \int_{-S}^S dz \left(1 - \frac{|z|}{S}\right) \frac{\xi(\mathbf{r})/\bar{\rho}^2}{D_z^{1/2}(\mathbf{r})} \exp\left[-\frac{v^2}{2D_z(\mathbf{r})}\right] \tag{C8}$$

while for a finite temperature we can cast Eq. (C7) in the form of convolution of the zero temperature correlation function with the thermal window

$$\xi_s(\mathbf{R}, v) \propto \int_{-\infty}^{\infty} \frac{dv'}{(4\pi\beta)^{1/2}} \exp\left[-\frac{(v - v')^2}{4\beta}\right] \int_{-S}^S dz \left(1 - \frac{|z|}{S}\right) \frac{\xi(r)}{D_z(\mathbf{r})^{1/2}} \exp\left[-\frac{v'^2}{2D_z(\mathbf{r})}\right] \quad . \tag{C9}$$

D. 1D, 2D AND 3D PPV POWER SPECTRA

Here we present short-wave asymptotics and useful approximations for the 1D, 2D and 3D PPV power spectra. One of the main formulas of LP00, Eq. (16) expresses the 3D PPV power spectrum through a 3D real space correlation function. Using the notation of the present paper this result can be written as

$$P_s(\mathbf{k}) \propto \int d^3\mathbf{r}\, e^{i\mathbf{KR}} \xi(r) \exp\left[-k_v^2 D_z(\mathbf{r})\right] \tag{D1}$$

In comparison with LP00, here $\mathbf{k} = (\mathbf{K}, k_v D_z^{1/2}(S)/S)$ and in the absence of coherent shearing motions (e.g., due to galactic rotation) the $3D$ plane wave is reduced to the $2D$ one. For the negative γ we integrate over the structure function $d(r)$ rather than the correlation function $\xi(r)$.

The one-dimensional spectrum along the velocity coordinate is

$$P_1(k_v) = \int d\mathbf{K} P_s(\mathbf{K}, k_v) \tag{D2}$$

$$\propto \int dz\, \xi(z) \exp\left[-k_v^2 D_z(S)(z/S)^m\right]$$

$$\propto (r_0/S)^\gamma \left[k_v D_z^{1/2}(S)\right]^{2(\gamma-1)/m} \tag{D3}$$

The result is valid for $\gamma < 1$. $P_1(k_v)$ coincides with $P_{nar}(k_v)$ in this paper.

The two-dimensional spectrum orthogonal to the line of sight is

$$P_2(K) = \int dk_v P_s(\mathbf{K}, k_v) \tag{D4}$$

$$\propto \int d^3\mathbf{r}\, e^{i\mathbf{KR}} \frac{\xi(r)}{r^{m/2}} - (regularization\ for\ \gamma + m/2 \le 1)$$

$$\propto -\frac{r_0^\gamma S^{m/2}}{D_z^{1/2}(S)} \int d^2\mathbf{R}\, e^{i\mathbf{KR}} \int dz \left[\frac{(R^2+z^2)^{1-\gamma/2+m/4}}{(1+m/2)R^2+z^2} - \frac{1}{z^{\gamma+m/2}}\right] \tag{D5}$$

$$\propto (r_0/S)^\gamma (KS)^{\gamma+m/2-3} \tag{D6}$$

The regularizing term that appears in Eq. (D5) is proportional to $\delta(\mathbf{K})$, thus not affecting the high wave number asymptotics. Its introduction is equivalent to taking the Fourier transform of $d_s(R) = 2(\xi_s(0,0) - \xi_s(R,0))$ rather than $\xi_s(R,0)$ to compute the $P_2(\mathbf{K})$. This definition is appropriate for shallow spectra $\gamma + m/2 \le 1$. The final asymptotics is valid for $\gamma + m/2 > -1$. For $1 < \gamma + m/2 < 3$ no regularization is necessary and asymptotic expression (D6) arises directly.

The spectra in orthogonal PPV directions, $P_1(k_v)$ and $P_2(K)$ look quite different. Let us however introduce the scaled velocity wavenumber $k_æ = S\left[k_v^2 D_z(S)\right]^{1/m}$ and correspondingly transformed PPV wavevector $\mathbf{k}_{PPV} = (\mathbf{K}, k_æ)$. The 1D spectrum in $k_æ$ coordinates is obtained from the condition of power conservation under variable change, $P_1(k_æ)dk_æ = P_1(k_v)dk_v = (D_z(S)/S^m)^{1/2}P_1(k_v[k_æ]) k_æ^{m/2-1}dk_æ$. Therefore,

$$P_1(k_æ) \propto (r_0/S)^\gamma (D_z(S)/S^m)^{1/2} [k_æ S]^{\gamma+m/2-2} \quad . \tag{D7}$$

With this variable change, correspondent to transformation in PPV space from v to z_v according to Eq. (50), the spectra exhibit the same scaling in both z_v and position coordinates (the difference by one is due to different dimensionality of spaces that P_1 and P_2 are defined on). This is the same relation that we have discussed for the structure functions in Section 3.5, however the language of spectra has an advantage that there is no issue with structure function saturation for $\gamma + 3m/2 < 1$.

The asymptotic scalings of all PPV spectra at high wavenumbers, including the one for 3D $P_s(\mathbf{K}, k_v)$ that we take from LP00, are summarized in Table D3. In this Table the two parts that 3D spectrum $P_s(\mathbf{k})$ splits into (see LP00)

$$P_s(\mathbf{k}) = P_v(\mathbf{k}) + P_\rho(\mathbf{k}) \quad , \tag{D8}$$

(where the part $P_v(\mathbf{k})$ depends only on the velocity statistics and the part $P_\rho(\mathbf{k})$ has contributions from both velocity and density), are presented separately.

REFERENCES

Armstrong, J. W., Rickett, B. J., & Spangler, S. R. 1995, ApJ, 443, 209
Ballesteros-Paredes, J., Klessen, R.S., Mac Low M., Vazquez-Semadeni E. 2006, in Protostars and Planets V, astro-ph/0603357
Beresnyak, A. & Lazarian, A., ApJL, 640, L175
Beresnyak, A., Lazarian, A., Cho, J. 2005, ApJ, 624, L93

Biskamp, D. 2003, Magnetohydrodynamical Turbulence (Cambridge, CUP)
Boldyrev, S. 2005, ApJL, 626, L37
Chepurnov, A. & Lazarian, A. 2006, MNRAS, in preparation
Cho, J., & Lazarian, A. 2003, MNRAS, 345, 325
Cho, J., & Lazarian, A. 2004, ApJ, 615, L41
Cho, J., & Lazarian, A. 2005, Theoretical and Computational Fluid Dynamics, 19, 127

1D: $P_s(k_v)$	2D: $P_s(K)$	3D: $P_s(K,k_v)$
$k_v D_z^{1/2}(S) \gg 1$	$KS \gg 1$	$k_v^2 D_z(S) \gg (kS)^m$
$P_\rho:\ (r_0/S)^\gamma \left[k_v D_z^{1/2}(S)\right]^{2(\gamma-1)/m}$	$(r_0/S)^\gamma [KS]^{\gamma+m/2-3}$	$(r_0/S)^\gamma \left[k_v D_z^{1/2}(S)\right]^{-2(3-\gamma)/m}$
$P_v:\quad\ \left[k_v D_z^{1/2}(S)\right]^{-2/m}$	$[KS]^{m/2-3}$	$\left[k_v D_z^{1/2}(S)\right]^{-6/m}$

TABLE D3
THE SHORT-WAVE ASYMPTOTIC BEHAVIOR OF POWER SPECTRA IN PPV SPACE.

Cho, J., & Lazarian, A. 2006, ApJ, 638, 811
Cho, J., Lazarian, A., Honein, A., Knaepen, B., Kassinos, S., & Moin, P. 2003, ApJ, 589, L77
Deshpande, A.A., Dwarakanath, K.S., & Goss, W.M. 2000, ApJ, 543, 227
Dickman, R. L., & Kleiner, S. C. 1985, ApJ, 295, 479
Elmegreen, B. 2002, ApJ, 577, 206
Elmegreen, B. & Falgarone, E. 1996, ApJ, 471, 816
Esquivel, A. & Lazarian, A. 2005, ApJ, 631, 320
Esquivel, A., Lazarian, A., Pogosyan, D., & Cho, J. 2003, MNRAS, 342, 325
Falgarone, E. 1999, in Interstellar Turbulence, ed. by J. Franco, A. Carraminana, CUP, (henceforth Interstellar Turbulence) p.132
Falgarone, E., Pineau Des Forets, G., Hily-Blant, P., & Schilke, P. 2006, astro-ph/0601607
Green, D.A. 1993, MNRAS, 262, 327
Heiles, C. & Troland, T.H. 2004, ApJS, 151, 271
Heyer, M. & Brunt, C. 2004, ApJ, 615, 45
Inogamov, N.A. & Sunyaev, R.A. 2003, Astronomy Letters, 29, 791
Kim, J., & Ryu, D. 2005, ApJ, 630, L45
Kleiner, S. C., & Dickman, R. L. 1985, ApJ, 295, 466
Larson, R. 2003, Reports on Progress in Physics, Volume 66, Issue 10, p. 1651
Lazarian, A. 1995, A& A, 293, 507
Lazarian, A. 2004, Journal of Korean Astronomical Society, 37, 563
Lazarian, A. 2005, BAAS, 207, 119.02
Lazarian, A. 2006a, ApJ, 645, L25
Lazarian, A. 2006b, Astron. Nachricht., 609, issue 5/6, 327
Lazarian, A. & Esquivel, E. 2003, ApJ, 592, L37
Lazarian, A., & Pogosyan, D. 2000, ApJ, 537, 72
Lazarian, A., & Pogosyan, D. 2004, ApJ, 616, 943
Lazarian, A., Pogosyan, D., & Esquivel, A. 2002, in ASP Conf. Ser. 276, Seeing Through the Dust, ed. R. Taylor, T. L. Landecker, & A. G. Willis (San Francisco: ASP),182
Lazarian, A., Pogosyan, D., Vázquez-Semadeni, E., & Pichardo, B. 2001, ApJ, 555, 130

Lazarian, A., Vishanic, E., Cho, J. 2004, ApJ, 603, 180
Lazarian, A. & Yan, H. 2004, in "Astrophysical Dust" eds. A. Witt & B. Draine, APS, V. 309, p.479
Maron, J. & Goldreich, P. 2001, ApJ, 554, 1175
McKee, Christopher F.; Tan, Jonathan C. 2002, Nature, 416, 59
Miesch, M. & Scalo, J. 1995, ApJL, 450, L27
Miesch, M. & Scalo, J. 1999, ApJ, 524, 895
Monin, A.S. & Yaglom, A. M. 1975, Statistical Fluid Mechanics: Mechanics of Turbulence, Vol. 2 (Cambridge: MIT Press)
Munch, G. 1958, Rev. Mod. Phys., 30, 1035
Narayan, R., & Goodman, J. 1989, MNRAS, 238, 963
Narayan, R., & Medvedev, M. 2001, ApJ, 562, L129
Ossenkopf, V., Esquivel, A., Lazarian, A., & Stutzki, J. 2006, A&A, 452, 2230
Padoan, P., Goodman, A.A., & Javela, M. 2003, ApJ, 588, 881
Padoan, P., Jimenez, R., Juvela, M. & Norlund, A. 2004, ApJ, L49
Pudritz, R. E. 2001, From Darkness to Light: Origin and Evolution of Young Stellar Clusters, ASP , Vol. 243. Eds T. Montmerle and P. Andre. San Francisco, p.3
Schlickeiser, R. 2002, Cosmic Ray Astrophysics, (Berlin: Springer)
Spangler, S.R., & Gwinn, C.R. 1990, ApJ, 353, L29
Stanimirović, S., & Lazarian, A., 2001, ApJ, 551, 53
Stutzki, J. 2001, Astrophysics and Space Science Supplement, 277, 39
Stutzki, J., Bensch, F., Heithausen, A., Ossenkopf, V., & Zielinsky, M. 1998, A&A, 336, 697
Sunyaev, R.A., Norman, M.L., & Bryan, G.L. 2003, Astronomy Letters, 29, 783
von Hoerner, S. 1951, Zeitschrift für Astrophysics, 30, 17
Wakker, B. 2004, Ap&SS, 289, 381
Wilson, O.C., Munch, G., Flather, E.M., & Coffeen, M.F. 1959, ApJS, 4, 199

Yan, H., Lazarian, A. & Draine, B. 2004, ApJ, 616, 895